



Stepwise candidate drug screening for myopia control by using zebrafish, mouse, and Golden Syrian Hamster myopia models

Meng-Yin Lin^{a,b,c}, I-Tsen Lin^d, Yu-Ching Wu^e, I-Jong Wang^{d,f,*}

^a Department of Ophthalmology, Taipei Medical University–Shuang Ho Hospital, Taipei, Taiwan

^b Institute of Clinical Medicine, College of Medicine, National Taiwan University, Taipei, Taiwan

^c Department of Ophthalmology, School of Medicine, Taipei Medical University, Taipei, Taiwan

^d Department of Ophthalmology, National Taiwan University Hospital, 7 Chung-Shan S. Rd., Taipei, Taiwan

^e Department of Medical Research, National Taiwan University Hospital, Taipei, Taiwan

^f Graduate Institute of Clinical Medical Science, China Medical University, Taichung, Taiwan

ARTICLE INFO

Article History:

Received 4 April 2020

Revised 15 November 2020

Accepted 11 February 2021

Available online xxx

Keywords:

Myopia

Zebrafish

C57BL/6 mouse

Golden Syrian hamster

MMP inhibitors

ABSTRACT

Background: We developed a preclinical protocol for the screening of candidate drugs able to control myopia and prevent its progression. The protocol uses zebrafish, C57BL/6 mice, and golden Syrian hamster models of myopia.

Methods: A morpholino (MO) targeting the zebrafish lumican gene (*zlum*) was injected into single-cell zebrafish embryos, causing excessive expansion of the sclera. A library of 640 compounds with 2 matrix metalloproteinase (MMP) inhibitors (marimastat and batimastat), which have the potential to modulate scleral remodelling, was screened to identify candidates for mitigating scleral diameter expansion in *zlum*-MO-injected embryos. The myopia-prevention ability of compounds discovered to have superior potency to inhibit scleral expansion was validated over 4 weeks in 4-week-old C57BL/6 mice and 3-week-old golden Syrian hamsters with form-deprivation myopia (FDM). Changes in the refractive error and axial length were investigated. Scleral thickness, morphology of collagen fibrils in the posterior sclera, messenger RNA (mRNA) expressions, and protein levels of transforming growth factor- β 2 (TGF- β 2), tissue inhibitor of metalloproteinase-2 (TIMP-2), MMP-2, MMP-7, MMP-9, and collagen, type I, alpha 1 (collagen α 1) were investigated in C57BL/6 mice, and MMP-2, MMP-9, and MMP activity assays were conducted in these mice.

Findings: In the zebrafish experiment, atropine, marimastat, batimastat, doxycycline, and minocycline were the drugs that most effectively reduced expansion of scleral equatorial diameter. After 28-day treatment in diffuser-wearing mice and 21-day treatment in lid-sutured hamsters, myopic shift and axial elongation were significantly mitigated by eye drops containing 1% atropine, 50 μ M marimastat, 5 μ M batimastat, or 200 μ M doxycycline. MMP-2 mRNA expression in mouse sclera was lower after treatment with atropine, marimastat, batimastat, or doxycycline. The protein levels and activity of MMP-2 and MMP-7 were significantly reduced after treatment with atropine, marimastat, batimastat, doxycycline, and minocycline. Furthermore, scleral thickness and collagen fibril diameter were not lower after treatment with atropine, marimastat, batimastat, or doxycycline than those of occluded eyes.

Interpretation: Stepwise drug screening in a range of models from *zlum*-MO-injected zebrafish to rodent FDM models identified effective compounds for preclinical myopia control or prevention. On the basis of the 640 compounds that were screened, MMP inhibitors may offer alternatives for clinical trials.

Funding: This research was supported by grants from Taiwan's Ministry of Science and Technology and Ministry of Health and Welfare.

© 2021 The Author(s). Published by Elsevier B.V. This is an open access article under the CC BY-NC-ND license (<http://creativecommons.org/licenses/by-nc-nd/4.0/>)

Introduction

Axially myopic eyes are characterised by increased axial length (AL) and thinning of the posterior sclera, [1] which mainly comprises interwoven lamellae of type I collagen fibrils and proteoglycans in humans and tree shrews [2]. In myopia, visual stimuli induce signalling from the retina via the retinal pigment epithelium (RPE) and

* Corresponding author at: Department of Ophthalmology, National Taiwan University Hospital, 7 Chung-Shan S. Rd., Taipei, Taiwan.

E-mail address:

Research in context

Evidence before this study

Myopia prevention in schoolchildren is a crucial public health issue. Pharmaceutical agents, increased outdoor activity, and orthokeratology have been shown to inhibit myopia progression and development. Currently, atropine, in eye drop form, is the only agent to have been used in this regard.

Added value of this study

Common features of studies have been that high-concentration atropine led to superior myopia control but had side effects, such as irritation, blurred vision, photophobia, cataract, loss of accommodation, and rebound after cessation. Low-dose (0.01%–0.05%) atropine eye drops, therefore, have become the main myopia treatment. However, finding other agents for preventing myopia progression without the side effects of atropine remains crucial. In the current study, we found that eye drops containing MMP inhibitors can significantly mitigate myopic shift and axial elongation in rodent FDM models after initial drug screening in zebrafish model.

Implications of all of the available evidence

Our preclinical stepwise drug screening in several models from *zlm*-MO-injected zebrafish to rodent FDMs identified effective compounds for preclinical myopia control or prevention. Based on the 640 compounds that were screened, MMP inhibitors may offer alternatives for clinical trials.

distribution was severely disrupted, and the phenotype resembled that of high myopia in humans; that is, increased AL, thin sclera, and retinal detachment [15]. Additionally, we demonstrated that knock-down of the zebrafish *lumican* (*zlm*) gene can cause scleral thinning and expansion of equatorial diameter, which are consistent with the features of high myopia in humans. This *zlm*-knockdown model can be further used as a drug screening protocol for identifying compounds that modulate scleral growth [16].

In clinical scenarios, pharmaceutical agents [17], increased outdoor activity [18], and orthokeratology [19] have been used to inhibit the progression or development of myopia [20]. The pharmaceutical agents atropine [21], pirenzepine [22], and 7-methylxanthine [23] and intraocular pressure-lowering agents [24] have been used in this regard. Atropine has had the most favourable results in preventing myopia progression in children [25]. However, the side effects of high concentrations of atropine in eye drops, such as irritation, blurred vision, photophobia, cataract, and solar retinopathy caused by mydriasis and loss of accommodation, limit its clinical applications [26]. Studies conducted in Singapore [namely Atropine in the Treatment of Myopia (ATOM), ATOM1, ATOM2, and ATOM3] have investigated 0.01% atropine for the treatment of myopia [27–28]. Given the promising results obtained for 0.01% atropine in ATOM2, many subsequent clinical trials have been designed to test low-dose atropine; the results, including those of a long-term study discovering minimal side effects and high efficacy [29], support the use of 0.01% atropine in clinical practice. A proposed study in Hong Kong regarding 0.01% atropine in combination with orthokeratology might yield illuminating results.[30] The Low-Concentration Atropine for Myopia Progression study conducted in Hong Kong in which low-concentration atropine was examined for myopia progression determined that in young children, 0.01% atropine achieved the optimal myopia-retarding effect with negligible side effects [31]. Common features of such studies have been that high-concentration atropine led to superior myopia control [31]; however, rebound myopia was observed after cessation of such a high-concentration treatment [25, 32–34]. Therefore, finding other potential agents to prevent myopia progression with few side effects and through other possible mechanisms remains crucial.

In this study, we broadened the spectrum of drug screening in search of a remedy with superior efficacy in *zlm*-knockdown zebrafish models and aimed to validate the efficacy of selected compounds to mitigate myopia progression in rodent models [35]. In addition, we compared the efficacy of selected MMP inhibitors with that of atropine in form-deprived (FD) eyes of C57BL/6 mice and golden Syrian hamsters because the efficacy of atropine eye drops in these animals is consistent with that for controlling myopia progression in humans.[29]

Methods

The animal research in this study was approved by the Institutional Animal Care and Use Committee of National Taiwan University and was performed in compliance with the Association for Research in Vision and Ophthalmology Statement for Use of Animals in Ophthalmic and Vision Research.

Zebrafish aquaculture

Zebrafish of the AB–Tuebingen strain, a hybrid cross of the AB and Tuebingen strains, were purchased from the Taiwan Zebrafish Core Facility at Taiwan's Academia Sinica. They were raised and maintained at 28°C under a 14–10-h light–dark cycle in accordance with established protocols [36]. Embryos were staged using morphological criteria (somite number) [37] and time since fertilisation. The embryos were generated through natural pair-wise mating, as described in the Zebrafish Book [38]. For each mating, 5 pairs were

choroid to facilitate scleral remodelling through modulating growth factors [3]. These growth factors activate matrix metalloproteinase (MMP) to modulate the synthesis and degradation of the extracellular matrix, alter mechanical tissue properties [4], increase creep rates [5], and cause increased AL and thinning of the posterior sclera [2, 6].

One study using a tree shrew model of myopia demonstrated that placing a minus lens in front of the eye produced axial elongation and a myopic shift and significantly upregulated the expression of membrane-type 1–MMP and MMP-2 messenger-RNAs (mRNAs), downregulated the expression of tissue inhibitor of metalloproteinase-3 (TIMP-3) mRNA, and induced a higher creep rate in the sclera [7]. Notably, elevated levels of aqueous MMP-2, TIMP-1, TIMP-2, and TIMP-3 were discovered in the aqueous humour when the axis was elongated [8]. Furthermore, MMP-2 level, but not MMP-3 level, was increased in the aqueous humour of individuals with strong myopia, and TIMP-1, -2, and -3 levels were positively and extremely significantly correlated with MMP-2 level [8]. The level of transforming growth factor (TGF)- β 2 was elevated in the aqueous humour of human myopic eyes [9]. In a chick myopia model, TIMP-2 mRNA expression was significantly reduced in the posterior sclera of eyes with form-deprivation myopia (FDM) [10]. In addition, the MMP-2 level increased during FDM development and decreased during recovery from myopia in tree shrews [11]. Zhao et al. identified a cause-and-effect relationship between MMP-2 upregulation and myopia development in fibroblast-specific MMP-2 knockout mice [12]. Therefore, the formation of axial myopia is strongly associated with the balance of MMP and TIMP activity in the sclera.

In addition to collagen, the scleral extracellular matrix contains small leucine-rich proteoglycans such as lumican, decorin, and keratan, which can regulate collagen fibrillogenesis; polymorphisms in the genes encoding these substances have been associated with myopia development in human genetics studies [13, 14]. In mice with both lumican and fibromodulin knockout, the collagen fibril diameter

prepared, and 200–300 embryos were generated. Chorions were removed manually using Dumont Watchmaker's No. 5 Forceps.

zlum knockdown through morpholino injection

We previously characterised *zlum* [16], and in this study, we designed and synthesised *zlum*-morpholino (MO; from Gene Tools, Philomath, OR, USA) to target the translation start codon of the respective gene. The oligonucleotide complemented the sequence from –8 through +17 with respect to the translation initiation codon as follows: 5'-GATCCCAGAGCAAACATGGCTGCAC-3'. A widely reported random-sequence MO (RS-MO), obtained from Gene Tools, was employed to serve as a control for *zlum*-MO; the RS-MO was 5'-CCTCTTACTCAGTTACAATTATA-3', which has been extensively used and for which few reports of off-target effects at reasonable doses have been published [39]. MO was resuspended in sterile water to a concentration of 1 mM and diluted to 680 ng/ μ L with sterile water. Solutions were prepared and injected into single-cell fertilised ova by using a Nanoject II auto-nanoliter injector and #3-000-203-G/XL replacement tubes (Drummond Scientific Company, Broomall, PA, USA) [16]. Injected embryos were maintained at 28°C until analysis.

To clarify the effect of *zlum* knockdown and establish the zebrafish model for myopia drug screening, the ratio of the RPE diameter to the sclera diameter was measured as the equatorial diameter in the horizontal plane and calculated in wild-type (WT), RS-MO-injected, *zlum*-MO-injected, and atropine-treated *zlum*-MO-injected embryos (Fig. 2d and 2e). The maximal sublethal concentration of atropine was determined as the highest one among concentrations, in which higher than 80% of embryos survived at 7 days postfertilisation (dpf) [16]. The embryos were placed in a 24-well plate (10 embryos per well) and exposed to 0.00%, 0.01%, 0.1%, 0.25%, 0.5%, and 1% atropine dissolved in double-distilled water. The drug screening protocol was shown in Fig. 2a. The compounds were added at 2 dpf and removed at 4 dpf. At 7 dpf, the dead larvae were counted and removed. The live embryos were anaesthetised with tricaine (Tricaine-S, Western Chemical, Ferndale, WA, USA), immobilised in 3% methylcellulose, and the ratios of the equatorial diameter in the live embryos were recorded. We finally selected 0.5% atropine for treating the *zlum*-MO-injected embryos as the concentration at which $\geq 80\%$ of embryos survived to 7 dpf. The data were analysed with Kolmogorov-Smirnov test as Normality test and Wilcoxon rank-sum test as nonparametric test. A significant difference was defined as $P < .05$.

Whole-mount in situ hybridisation

Zebrafish embryos were obtained at various stages of growth and fixed in 4% paraformaldehyde in phosphate-buffered saline (PBS; pH 7.4; Invitrogen Life Technologies, Carlsbad, CA, USA) overnight at 4°C. After three rinses with PBS, we transferred the embryos into 100% methanol and stored them at –20°C until use. All embryos were treated with 0.003% phenylthiourea (Sigma, St. Louis, MO, USA) to prevent melanogenesis in the skin. Whole-mount in situ hybridisation was performed to identify *zlum* mRNA by using a previously described protocol [40]. The oligonucleotide sequence (5'-3') was GTTCCATCCAAGCGCAGGGTCTCAGTCTAGAGTAGTTGACCGGT-GAGCTAAATCTGCA. The hybridisation signals were visualised with anti-digoxigenin antibody conjugated with alkaline phosphatase by using a procedure recommended by Roche Applied Science (Indianapolis, IN, USA). Images were obtained using an AxioCam digital camera on a dissecting microscope (Zeiss, Germany).

Immunohistochemistry

To develop an anti-*zlum* antibody (Blossom Biotechnologies, Taiwan), we generated an affinity-purified antibody against the immunising N-terminal peptide (N'-CNERNLKFIVPTGIKY-C')

corresponding to the 18 N-terminal amino acid residues inferred from *zlum* cDNA to detect zebrafish lumican. The peptides were conjugated to keyhole limpet haemocyanin for antibody production in rabbits [16]. Zebrafish embryos were fixed, as described above, with 4% paraformaldehyde in PBS. After they were washed with PBS, they were incubated with 0.5 units/mL keratanase at 37°C overnight. Then, the samples were blocked with 3% hydrogen peroxide for 30 min, incubated with the previously produced anti-zebrafish lumican antibody (0.1 μ g/mL) that had been purified with SulfoLink gel conjugated against the immunising N-terminal lumican peptide for 16 h at 4°C [16], washed with PBS for 3 times (10 min/each time) at room temperature, and then incubated with Alexa Fluor 488 goat anti-rabbit immunoglobulin G (Invitrogen, Carlsbad, CA, USA) for 1 h at room temperature. Prior to observation, the samples were incubated with 4',6'-diamidino-2-phenylindole (Sigma, St. Louis, MO, USA) for 10 min. We obtained negative control samples by using primary antibody, which preabsorbed the immunogen in a molar ratio of 10:1 (peptide to antibody) overnight at 4°C.

Food and drug administration—approved compound library used for primary drug screening

We employed the *zlum*-knockdown embryos in the study experiments. To ensure a wide scope of drug screening, a US Food and Drug Administration (FDA)-approved commercial drug library (Enzo Life Sciences, Farmingdale, NY, USA) was employed. This library consists of 640 FDA-approved drugs carefully selected to maximise chemical and pharmacological diversity. MMPs have been demonstrated to regulate scleral remodelling during myopia development [7, 12, 41]. Therefore, we compared the inhibition potency of two potent MMP inhibitors, namely batimastat and marimastat, with that of other compounds. First, *zlum*-MO was microinjected into single-cell-stage embryos under a dissecting microscope, and the embryos were then exposed to drugs at 2 dpf. Each time, more than 50 embryos were treated with one drug for 48 h at 28.5°C. For each drug, the procedure was repeated at least three times with different groups of 50 embryos each. At 7 dpf, the ALs of eyeballs and percentage of scleral tissue expansion for each compound were recorded as described in our previous study.[16] The sclera was considered expanded when the equatorial diameter of RPE was less than half of the equatorial diameter of sclera. Inhibition potency, which represents the ability of a drug to reduce the percentage of morphants with expanded scleral equatorial diameter, was defined and calculated as follows.

$$\left[\frac{\text{(number of morphants with expanded scleral equatorial diameter after treatment with a specific compound - number of morphants with expanded scleral equatorial diameter without treatment)}}{\text{number of morphants with expanded scleral equatorial diameter without treatment}} \right] \times 100\%$$

Selection of candidate compounds

In our search for candidate compounds that reduce scleral tissue expansion, the compounds that exhibited the highest potency for inhibiting scleral expansion and those involved in the relevant mechanisms of collagen degradation and synthesis—such as MMP inhibitors, TGF- β agonists, cyclooxygenase inhibitors, lipoxygenase inhibitors, statin derivatives, and angiotensinogen-converting enzyme inhibitors—were selected, and their individual effects on *zlum*-MO-induced expansion of scleral diameter were determined. The initial concentrations of these compounds were selected on the basis of those used in our previous study and others [16, 42, 43]. The optimal concentration was defined as that producing a survival rate similar to that for untreated morphants.

The treatment timeline of *zlum*-MO-injected embryos exposed to the selected compounds is illustrated in Fig. 2a. On each occasion, more than 100 embryos were treated with a drug, and an equivalent

number of internal controls was always prepared. For each compound, this procedure was repeated at least three times, and the percentage of scleral tissue expansion was calculated for each compound. The results were analysed using a normality test, and the median percentage for each compound was determined and compared using the nonparametric Dunn's test.

C57BL/6 mice myopia model

C57BL/6 mice were obtained from BioLASCO Co. (Yilan, Taiwan) and maintained in the Animal Breeding Unit at National Taiwan University College of Medicine. All mice were raised on a 12-h light–dark cycle. Before treatment began, mice with an interocular AL difference of more than 0.1 mm were excluded. A frosted hemispherical plastic diffuser, with a cap comprising a 0.5-mL polymerase chain reaction (PCR) tube (Scientific Specialties, Lodi, CA, USA), was sutured around the right eye of each mouse 4 weeks of age by using 6-0 nylon as previously described but with some modifications (Fig. 4a) [44, 45]. A hole was drilled in the cap to allow the instillation of eye drops by using a pipette. Collars made from thin plastic were fitted around the neck to prevent the mice from removing their diffuser. To prepare the eye drop solution, atropine, doxycycline, and minocycline were diluted in PBS, and marimastat and batimastat were dissolved in dimethyl sulfoxide (0.05%) and diluted with PBS. The five compounds that exhibited the highest potency for inhibiting scleral expansion (atropine, batimastat, marimastat, doxycycline, and minocycline) in the zebrafish candidate selection experiment were used; 1% atropine sulphate was adopted in accordance with previous murine studies [46–47]. For the other four compounds, we began with concentrations determined according to the results of the zebrafish experiment. We then titrated concentrations of 0.05, 0.5, 5, 20, 50, 100, 200, 500, and 1000 μM for marimastat, batimastat, doxycycline, tetracycline, captopril, minocycline, N-acetylcysteine, propofol, and aspirin to identify the concentration with the optimal inhibition potency in form-deprived (FD) C57BL/6 mice ($n=5$). Eventually, six groups of mice ($n=10$) were assigned to PBS, 1% atropine, 50 μM marimastat, 5 μM batimastat, 200 μM doxycycline, and 50 μM minocycline treatment. The tested compounds were instilled into the FD right eye, and PBS was instilled into the left eye. The instillation of compounds was initiated on 29 dpf (day 1 of instillation) and ended on 56 dpf (day 28 of instillation) twice every day (8 o'clock in the morning and 16 o'clock in the afternoon). A single eye drop (50 μL) completely filled the diffuser and induced a blink reflex to ensure that the eye drop had reached the cornea.

Refraction and AL were measured at day 0 (no instillation) and day 14 and 28 (after instillation) at 17 o'clock in the afternoon. Before measurement, the diffuser was removed by cutting periocular 6-0 nylon except on day 0. Each eye received instillation of 1% tropicamide ophthalmic solution (Alcon Laboratories, Inc., Fort Worth, TX, USA) three times at intervals of 5 minutes to ensure mydriasis and cycloplegia. Mice were anaesthetised with an intramuscular injection of 0.01 mL of tiletamine/zolezepam (50 mg/mL; Zoletil 50 Virbac S.A., Carros, France) and 0.01 mL of xylazine hydrochloride (23.32 mg/mL; Rompun, Bayer, Leverkusen, Germany). Refraction was measured using a streak retinoscope (Neitz, Japan) in darkness and at a working distance of 50 cm by using lens bars to neutralise the two principal meridians. Each time we took measurements in a mouse, the observer was blinded to the mouse's group, and three independent measurements were performed for each eye. The mean of three measurements was taken as the refractive error for further analyses. Moisture in the cornea was maintained through frequent PBS application by using a pipette. Overflow was removed using a cotton swab to ensure the precise detection of corneal curvature.

Under the same anaesthesia procedure, AL was measured through ultrasound biomicroscopy (Prospect High Resolution Imaging System, S-Sharp Corporation, Taipei, Taiwan) by using a probe that

produced a central frequency of 50 MHz. During measurement, the mouse was placed on a small elevated platform, and its neck was gently restrained between two cotton balls. To enhance signal transduction and clarity, the fur around the eyes was shaved, and a generous amount of gel was applied to the front of the eyeballs. To ensure that the axis of AL measurement was undeviated, the captured images were required to contain the pupil and shadow of the optic nerve. The AL was defined as the distance from the corneal epithelium to the front surface of the retina around the optic nerve. Each time we recorded measurements in a mouse, the observer was blinded to the mouse's group, and three independent measurements were performed for each eye. The mean of three measurements was taken as the refractive error for further analyses. After measurement, the diffuser was replaced by suturing with 6-0 nylon to the periocular skin except on day 0 and day 28 of instillation.

After every instillation for 28 days, the animals were euthanised by asphyxiation in 100% CO₂ [48]. Both eyeballs were enucleated, and the extraocular muscles and other adherent tissues outside the eyeballs were removed quickly under a surgical microscope (Carl Zeiss, OPMI pico, Germany). The eyeballs were then placed in cold PBS and photographed within 5 min of enucleation. A freshly excised eye was carefully placed on a platform and submerged in PBS with its anterior–posterior axis perpendicular to the video camera. Eyeball length was then measured using photographs taken by the camera and analysed using Image-Pro Plus version 4.5. According to the schematic eye model [49], the highly magnified video camera provided an estimated axial resolution of approximately 2.46 D (16 $\mu\text{m}/\text{pixel}$) [49].

Golden Syrian hamster myopia model

In addition, we validated the selected compounds in a golden Syrian hamster model for myopia. Three-week-old male golden Syrian hamsters were obtained from the National Laboratory Animal Center, Taipei, Taiwan. Hamsters with an AL of 3.99 to 4.05 mm were identified and reared under a 12-h light–dark cycle. On postnatal day 21, the right eyelid was sutured to induce FDM as previously described [50]. Subsequently, 1% atropine, 50 μM marimastat, 5 μM batimastat, or 200 μM doxycycline was instilled twice (8 o'clock in the afternoon 16 o'clock in the afternoon) per day for 21 days. The refractive error and AL were measured before treatment (postnatal day 21) and after 21 days of treatment (at 17 o'clock in the afternoon, postnatal day 42). A single eye drop (50 μL) was instilled into the palpebral fissure while we pulled the sutured eyelids slightly open with fingers, a blink reflex was induced to ensure that the eye drop had reached the cornea. Each time we recorded measurements for a hamster, the observer was blinded to the hamster's group, and three independent measurements of refractive error and AL were performed for each eye. The change between the two time points was calculated. The methods for measuring the AL and refractive error were the same as those used for the C57BL/6 mice.

Haematoxylin and eosin staining

The whole enucleated eyeballs were fixed in 4% paraformaldehyde in PBS overnight, serially dehydrated, embedded in paraffin, and sectioned at 6 μm . We stained 20 sections with haematoxylin and eosin (H&E). The general morphology of the posterior sclera and areas of the sclera–choroid junctions was examined.

Transmission electron microscopy

The enucleated mouse eyes were fixed in 2.5% glutaraldehyde and 2% paraformaldehyde in 0.1 M cacodylate buffer (pH 7.0) at 4°C overnight. The scleral tissues were separated and postfixed in 1% osmium tetroxide for 1 h, washed 3 times for 5 min in 0.1 M sodium cacodylate, washed 3 times in distilled water, dehydrated in 75% ethanol for

15 min, 80% ethanol for 15 min, 90% ethanol for 15 min, and 95% ethanol for 15 min twice and 100% ethanol for 15 min thrice sequentially, after which they were embedded in Araldite-Embed 812 resin (Electron Microscopy Sciences, Hatfield, PA, USA). Ultrathin 80-nm sections were subsequently cut using a diamond knife on a Leica EM UC7 ultramicrotome and stained with 2% aqueous uranyl acetate. Images were captured using transmission electron microscopy (TEM; JEOL JEM-1400, Peabody, MA, USA) at 75 keV. For the posterior sclera, micrographs of the central portion of the sclera wall were captured at 60 000 × magnification [16].

Measurement of scleral thickness and collagen fibril diameters

Collagen fibril diameter and scleral thickness were measured using Image-Pro Plus version 4.5 as previously described [16]. In the fibril diameter analysis, 12 micrographs of corresponding posterior sclera from 6 mice in each group were taken. We measured 6 non-overlapping regions in each micrograph, which generated 600 measurements for each group. In the scleral thickness analysis, 24 H&E-stained slices from 6 mice from each group were collected. Measurements were recorded around the optic nerve, and 72 measurements were generated for each group. The data of each group were compared with the data of PBS-treated eyes and analysed using independent sample *t* tests and the Bonferroni correction.

Quantitative real-time reverse transcription PCR

The mouse eyes were enucleated meticulously under a surgical microscope (Carl Zeiss, OPMI pico, Germany). The extraocular muscles and soft tissues were gently removed from the eyeballs with forceps, and an incision was made along the equator to separate the anterior and posterior segments, and anterior segments were discarded. Then, the cornea, lens, iris, ciliary body, RPE, retina, and vitreous humour were gently removed from the sclera using a spatula. We employed TRIzol Reagent (Life Technologies, Shanghai, China) to extract total RNA from the sclera. The RNA pellets were washed with cold 70% ethanol and dissolved in diethyl-pyrocyanate-treated water. Reverse transcription was conducted using SuperScript IV VILO Master Mix (Invitrogen; Thermo Fisher Scientific, Inc., Carlsbad, CA, USA) and total RNA (2 µg). To verify the gene expression of TGF-β2, TIMP-2, MMP-2, MMP-9, and collagen Iα1, quantitative real-time reverse transcriptase (qRT)-PCR was performed using iQ SYBR Green Supermix (Bio-Rad, Montreal, Canada). Each PCR reaction mixture contained 10 µL of SYBR Green Supermix, 4 µL of cDNA, and 1 µL of specifically designed primer sequences at a concentration of 2.5 µM. The cycling conditions were as follows: 95°C for 2 min; 40 cycles at 95°C for 5 s; and the optimal primer temperature for 30 s. Glyceraldehyde 3-phosphate dehydrogenase (*GAPDH*) was used as the internal control gene for reference, and mRNA levels of tested genes were standardised against it.

Western blotting

Total proteins were extracted from the whole zebrafish embryos (at 3 dpf) and the sclera of enucleated eyes of C57BL/6 mice in radioimmunoprecipitation assay (RIPA) buffer (50 mM Tris-HCl, pH 7.4, 150 mM NaCl, 1 mM ethylenediaminetetraacetic acid, 1% Na-deoxycholate, 1% NP-40; Pierce Biotechnology, Rockford, IL, USA) containing protease inhibitors (0.5 mM 4-(2-aminoethyl)benzenesulfonyl fluoride hydrochloride, 0.3 µM aprotinin, 10 µM bestatin, 10 µM E-64, and 10 µM leupeptin; Roche, Mannheim, Germany). A total of 100 zebrafish embryos of individual phenotypes with or without treatment and two to three mouse sclera of individual treatments were separately sonicated in 100 µL of RIPA buffer and then micro-fused for 20 min, after which the samples were homogenised on ice. Tissue debris was removed through centrifugation for 10 min at

10 000 rpm. The supernatant was saved, and its protein concentration was determined using Bio-Rad Dye Reagent (Bio-Rad, 500-0006). Prior to sodium dodecyl sulphate-polyacrylamide gel electrophoresis (SDS-PAGE), aliquots of some scleral protein extracts were digested with 0.1 units/mL endo-β-galactosidase (catalogue number 345811-50UL, Sigma) at 37°C overnight to remove poly-N-acetyllactosamine structures. We loaded 60 µg of protein sample without signal saturation and in the linear dynamic range. The clear supernatant proteins were resolved using SDS-PAGE (30 g per lane) in 10% polyacrylamide gel and transferred to a nitrocellulose membrane with a pore size of 0.2 µm (Invitrogen, Carlsbad, CA, USA) for immunoblotting. Zebrafish lumican was probed with the anti-zebrafish lumican N-terminal peptide antibody (0.1 µg/mL) as described previously. [16] We also used antibodies to other scleral proteins to evaluate the effects of *zlum* knockdown, and all these antibodies were obtained from commercial suppliers. The type, catalogue number, and source of the primary antibodies used in the zebrafish and mice are listed in supplemental Tables 1 and 2. Anti-rabbit (1:1000) and anti-goat (1:2500) horseradish peroxidase (HRP)-conjugated secondary antibodies were used with the appropriate primary antibodies. Antibody reactivity was detected through chemiluminescence (Immobilion Western HRP and AP Chemiluminescent). The relative band intensity was analysed using LabWorks software (v. 4.6; UVP Bioimaging Systems, Upland, CA, USA). The relative expression of an individual protein to that of *GAPDH* in each group of mice was also calculated.

MMP-2, MMP-9, and MMP activity assays

The activity of MMP-2, MMP-9, and MMPs (MMP-1, 2, 3, 7, 8, 9, 12, 13, and 14) in the sclera of enucleated eyes of C57BL/6 mice were quantified through an enzyme-linked immunosorbent assay (ELISA), as previously described [51–52]. In brief, the generic assay for activity of the several types of MMP (MMPs) employed Anaspec (San Jose, CA, USA) MMP assay kits. These assays measure the content of enzymatically active MMP as the amount of 5-FAM fluorophore released from a synthetic MMP substrate, detected fluorometrically. We employed a generic assay for several types of MMP (MMPs) (Anaspec, Cat. No. 71158), and type-specific assays for MMP-2 (Cat. No. 72224) and MMP-9 (Cat. No. 72017); procedures followed the manufacturer's instructions, and scleral extracts were incubated with the assay mixture at room temperature (20 deg C). For generic MMPs, the fluorescence intensity of a sample containing 1 µg/mL protein was measured every 5 min for 30–60 min after beginning the assay. For MMP-2 and MMP-9, 100 µg/mL samples were incubated in darkness. The fluorescence generated by MMP-2 activity was measured after incubation for 18 h; whereas that generated by MMP-9 activity was measured continuously, and data were collected every 10 min for 60–120 min after initiating the reaction. IC₅₀ values were obtained through dose–response measurements in a cytotoxic assay [53].

Statistical analysis

All data were identified as normally or non-normally distributed by using the Kolmogorov–Smirnov test. If the data were non-normally distributed, the data of each group is presented as median ± interquartile range (IQR) and analysed using the Wilcoxon rank sum test. If the data were normally distributed, they are presented as the mean ± standard deviation (SD). Multiple comparisons of groups were performed using either an analysis of variance (ANOVA) and the post hoc test or Student's *t* test with the Bonferroni correction. *P* < .05 indicated a statistically significant difference. The repeated measurement variability is presented as the intraclass correlation coefficient (ICC), which was regarded as favourable when it was between 0.75 and 0.90 [54]. The ICC was appropriate for measuring both refraction (ICC = 0.85) and AL (ICC = 0.79) in mice.

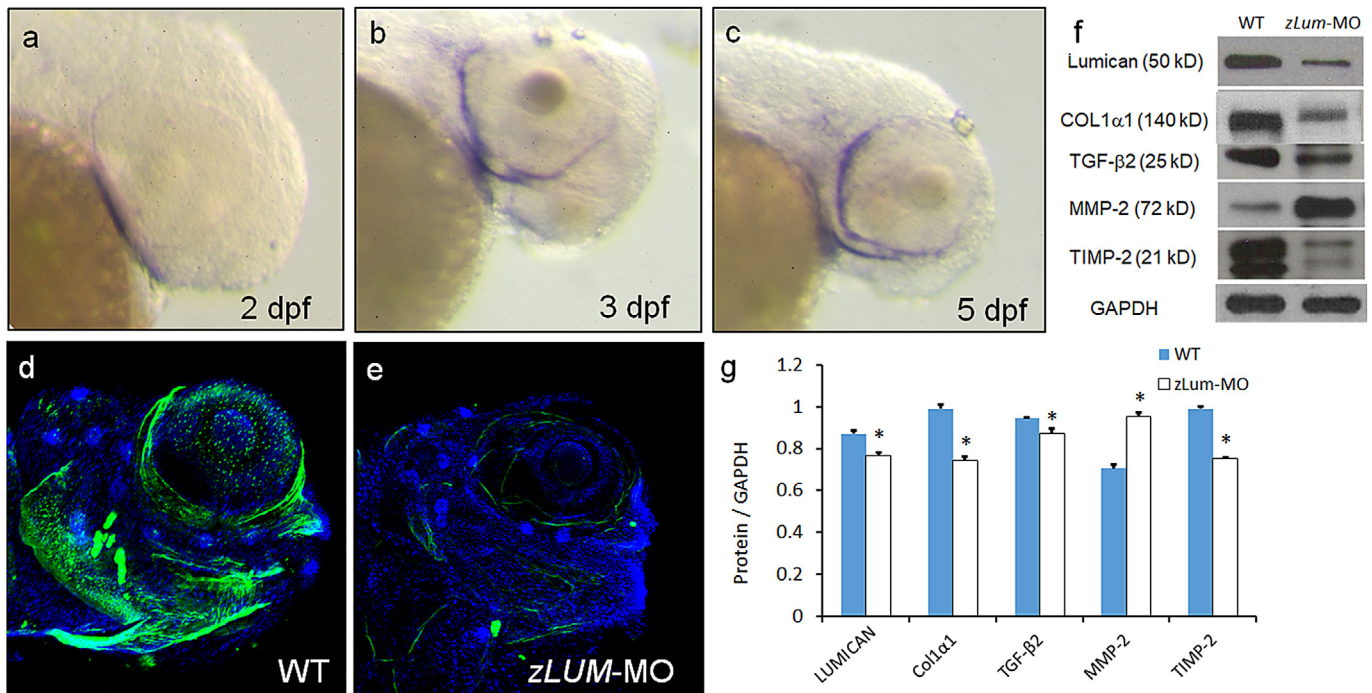


Fig. 1. Expression of lumican in zebrafish embryos. (a–c) *zlum* mRNA expressed in the sclera from 3 dpf by whole-mount in situ hybridisation. (d and e) Immunohistochemistry of lumican protein in WT and *zlum*-MO-injected embryos at 5 dpf; the *zlum*-MO-injected embryos exhibited markedly reduced lumican expression. (f) Western blot of WT and *zlum*-MO-injected embryos. (g) Histogram depicting the content of scleral proteins normalized to that of GAPDH in WT and *zlum*-MO-injected embryos ($n = 5$ per group). PDI, protein disulphide isomerase; GAPDH, glyceraldehyde-3-phosphate dehydrogenase.

Role of funders

The funders had no role in the writing of the manuscript or the decision to publish. The authors have not been paid to write this article by any agency.

Results

Spatial distribution of lumican mRNA and protein in zebrafish embryos

We used whole-mount in situ hybridisation to analyse the expression pattern of zebrafish lumican mRNA in zebrafish eyeballs during embryonic development. In WT embryos, lumican mRNA expression was first detected in the sclera at 3 dpf. The expression had extended to the entire sclera by 5 dpf (Fig. 1a–c). By contrast, the control sense riboprobes exhibited negligible hybridisation signals. Immunohistochemistry revealed that the expression of lumican protein in WT zebrafish eyeballs was similar to that of human lumican protein [55], which is mainly distributed in the cornea and sclera (Fig. 1d). However, in the *zlum*-MO-injected embryos, the expression of lumican protein was remarkably reduced (Fig. 1e).

Western blotting for WT and *zlum*-knockdown zebrafish

Fig. 1f presents western blots of lysates from zebrafish eyeballs with and without *zlum*-MO microinjection and then subjected to Western blotting analysis. The amount of each protein expression in relation to the amount of GAPDH (amount MMP / amount GAPDH), and the differences in amount of any protein, in scleras from WT vs *zlum*-MO fish, were expressed as fold difference. The fold difference in lumican/GAPDH protein expression in WT and *zlum*-MO zebrafish was 0.87 ± 0.02 and 0.77 ± 0.02 ($P = .01$), respectively; that of TGF- β 2/GAPDH was 0.95 ± 0.01 and 0.87 ± 0.02 ($P = .02$); that of TIMP-2/GAPDH was 0.99 ± 0.01 and 0.75 ± 0.01 ($P = .001$); that of MMP-2/

GAPDH was 0.71 ± 0.02 and 0.95 ± 0.02 ($P = .008$); and that of collagen α 1 /GAPDH was 0.99 ± 0.02 and 0.74 ± 0.02 ($P = .0003$; Fig. 1g; supplemental Fig. 1), respectively. These results indicated that the *zlum*-MO-injected embryos contained relatively high levels of MMP-2 protein and relatively low levels of lumican, TIMP-2, TGF- β 2, and collagen α 1 proteins.

Effects of *zlum* knockdown on equatorial diameter of sclera in zebrafish embryos

We microinjected *zlum*-MO into fertilised zebrafish eggs at the 1–4-cell stage. The effect of *zlum*-MO injection with or without addition of 0.5% atropine on scleral expansion is displayed in Fig. 2b. A significant increase in the scleral equatorial diameter of the *zlum*-MO-injected embryo compared with that of the RS-MO-injected embryo was observed at 7 dpf, but no difference was noted in eyeball size between the RS-MO and WT embryos (Fig. 2b). The ratios of the equatorial diameter of the RPE to the equatorial diameter of scleral tissue were nonnormally distributed (Kolmogorov–Smirnov test, $P < .01$). The ratio for each group is presented as the median \pm IQR and was analysed using the Wilcoxon rank sum test (Fig. 2b). WT (Fig. 2c) and RS-MO-injected (Fig. 2d) embryos had the same ratio (0.96 ± 0.03 , $P = 1$). Consequently, the ratio of the equatorial diameter of the RPE to the equatorial diameter of scleral tissue was significantly lower in the *zlum*-MO-injected group than in the RS-MO-injected and WT groups. In addition to enlarged eyeballs, enlarged pericardium and malformed body shape were noted at 7 dpf, as found in our previous study.[16] Compared with the WT embryos, the *zlum*-MO-injected embryos exhibited a significantly lower ratio (0.49 ± 0.06 , $P = .01$). Compared with the *zlum*-MO-injected embryos (Fig. 2e), the atropine-treated *zlum*-MO-injected embryos had a greater ratio (0.70 ± 0.14 , $P = .02$; Fig. 2f). This indicated that *zlum*-MO injection caused significant scleral expansion, which is similar to the morphological change that naturally occurs in human myopic eyes.[56] However, this scleral expansion could be prevented by the addition of 0.5%

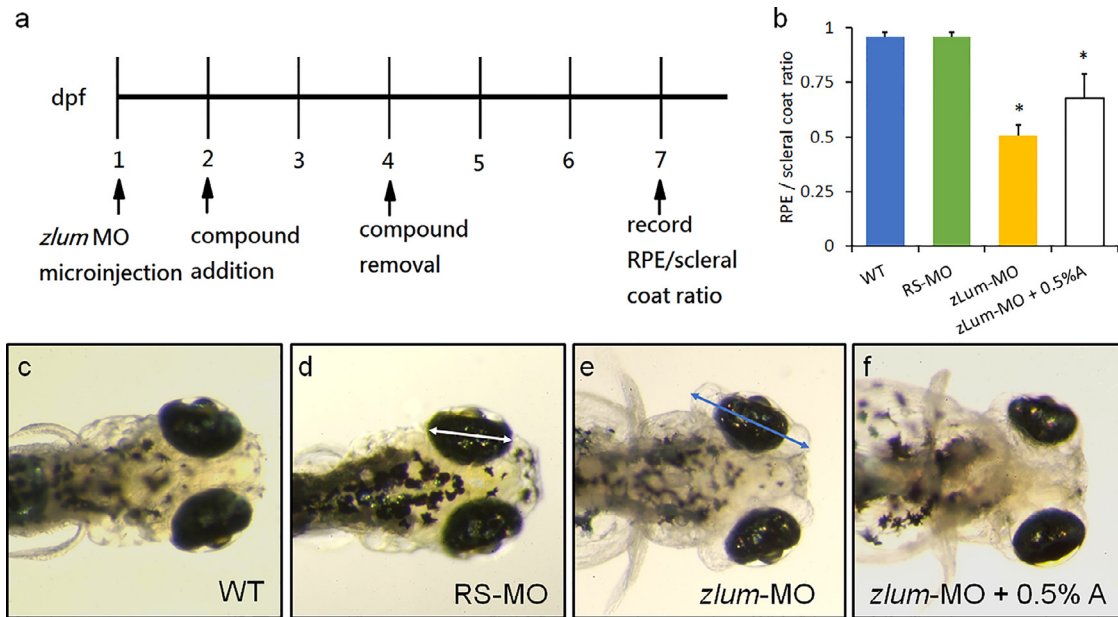


Fig. 2. *zlum*-Knockdown zebrafish as an *in vivo* model for screening compounds for myopia treatment. (a) Timeline of drug screening. (b) Histogram of the median \pm IQR of the ratio of the equatorial diameter of the RPE (white arrow) to the equatorial diameter of scleral tissue (blue arrow). The ratio in the *zlum*-MO-injected embryos (0.49 ± 0.06) was significantly increased with the addition of 0.5% atropine (0.70 ± 0.14 , Wilcoxon rank sum test, $P = .02$; $n = 5$). (c) WT embryo, (d) RS-MO embryo, (e) *zlum*-MO-injected embryo, and (f) *zlum*-MO-injected embryo with the addition of 0.5% atropine at 7 dpf.

atropine, which is consistent with our observations in human myopic eyes after dosing with atropine.[27]

Drug screening in zlum-MO-injected zebrafish embryos by using the FDA-approved compound library

Among the 640 FDA-approved compounds, 425 drugs and 2 MMP inhibitors, namely marimastat and batimastat (Fig. 3a), mitigate scleral diameter expansion. Among them, 11 compounds with an effect comparable to that of 0.5% atropine were investigated. The percentage ($<15\%$) of embryos with scleral expansion after treatment with PBS ($29.0\% \pm 4.3\%$), 0.5% atropine ($9.1\% \pm 4.0\%$), 50 μ M marimastat ($2.4\% \pm 2.5\%$), 5 μ M batimastat ($1.7\% \pm 0.7\%$), 200 μ M doxycycline ($3.8\% \pm 2.1\%$), 0.5 mM tetracycline ($5.0\% \pm 0.9\%$), 1 mM captopril ($6.25\% \pm 1.9\%$), 50 μ M minocycline ($6.7\% \pm 2.0\%$), 10 mM losartan ($10.0\% \pm 7.9\%$), 50 mg/L aspirin ($11.3\% \pm 6.0\%$), 50 μ M CL-82198 ($15.2\% \pm 1.3\%$), 50 μ M N-acetylcysteine ($15.6\% \pm 1.3\%$), and 0.5 mM propofol ($15.4\% \pm 5.4\%$) is expressed as the median \pm IQR in Fig. 3b. The Kruskal–Wallis test revealed that $P < .001$; thus, a post hoc test (Dunn’s test) was performed, revealing that batimastat, marimastat, doxycycline, and minocycline had effects comparable to that of 0.5% atropine in mitigating scleral diameter expansion (all $P < .05$).

Refraction and AL change in C57BL/6 mouse and golden Syrian hamster myopia models

The mitigating effect of each compound is expressed as the difference in refractive error (in units of dioptres, D) between the FD eye with treatment and unoccluded control eye of each mouse. Before treatment, the interocular differences were 0.07 ± 1.06 D in PBS-treated, -0.10 ± 1.47 D ($P = .77$) in 1% atropine-treated, -0.35 ± 1.03 D ($P = .478$) in 50 μ M marimastat-treated, 0.10 ± 1.78 D ($P = .962$) in 5 μ M batimastat-treated, 0.05 ± 1.26 D ($P = .849$) in 200 μ M of doxycycline-treated, and 0.56 ± 0.70 D ($P = .401$) in 50 μ M minocycline-treated FD eyes. After 28 days of treatment, the interocular differences between individual groups and the PBS-treated mice determined using independent sample *t* tests and the Bonferroni correction were 9.35 ± 1.51 D for the PBS-treated, 5.36 ± 1.25 D ($P < .01$) for the 1% atropine-treated, 4.45 ± 1.46 D ($P < .01$) for the 50

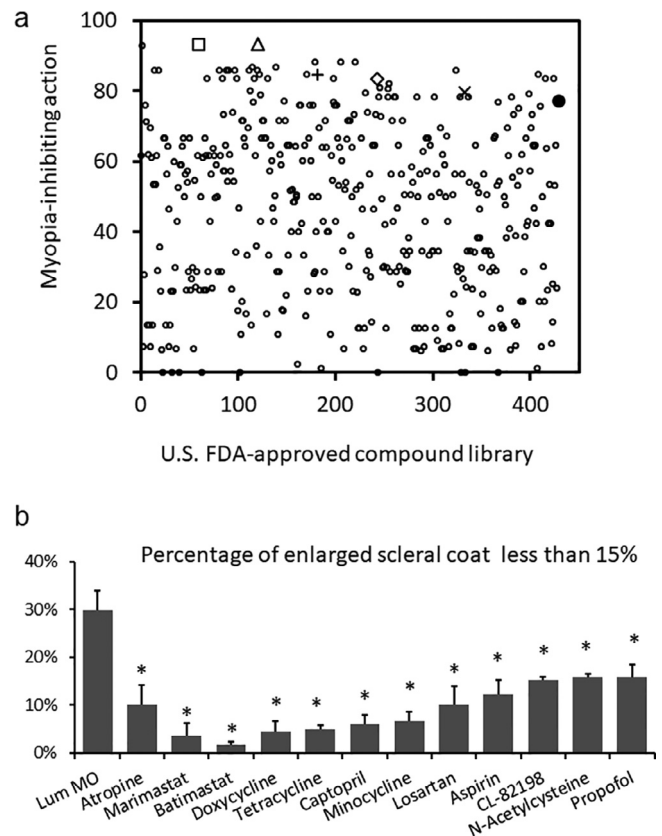


Fig. 3. Large-scale screening with *zlum*-knockdown zebrafish by using the FDA-approved drug library. (a) Plot presenting 427 compounds with positive myopia-inhibiting potency (δ : marimastat, Δ : batimastat, $+$: minocycline, \diamond : tetracycline, \circ : losartan, and \circ : doxycycline). (b) Compounds that can reduce the percentage of scleral tissue expansion to less than 15%: 0.5% atropine, 50 μ M marimastat, 5 μ M batimastat, 200 μ M doxycycline, 0.5 mM tetracycline, 1 mM captopril, 50 μ M minocycline, 10 mM losartan, 50 mg/L aspirin, 50 μ M CL-82198, 50 μ M N-acetylcysteine, and 0.5 mM propofol ($n = 300$, for each compound; the percentage of embryos with expanded scleral tissue is presented as median \pm IQR and analysed using Dunn’s test; $*P < .05$).

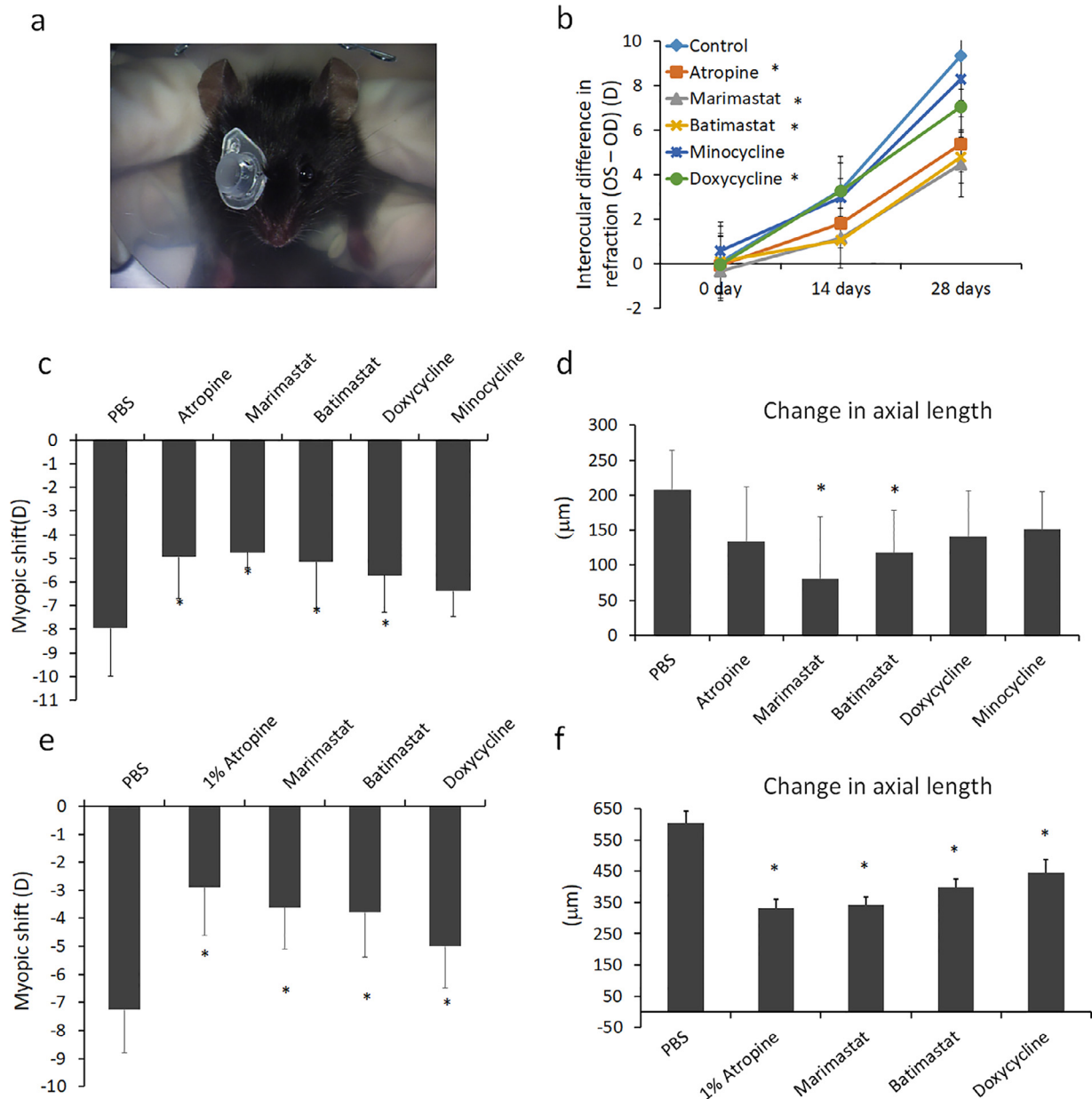


Fig. 4. FDM models of C57BL/6 mice and golden Syrian hamsters. (a) A 4-week-old C57BL/6 mouse wearing a plastic diffuser and collar. Instillation with 1% atropine, 50 μ M marimastat, 5 μ M batimastat, 200 μ M doxycycline, or 50 μ M minocycline. (b) Significantly reduced interocular refractive difference in C57BL/6 mice treated with marimastat, batimastat, atropine, or doxycycline as compared with their untreated fellow eyes. (c) Significantly reduced myopic shift of treatment in FD eyes of C57BL/6 mice treated with marimastat, batimastat, atropine, or doxycycline. (d) Significantly reduced axial elongation from the beginning to the end of FD eyes in C57BL/6 mice treated with marimastat, batimastat, atropine, and doxycycline ($n = 10$). (e) Significantly retarded myopic shift from the beginning to the end in FD eyes of golden Syrian hamsters treated with marimastat, batimastat, atropine, or doxycycline. (f) Significantly impeded axial elongation from the beginning to the end in FD eyes of golden Syrian hamsters treated with marimastat, atropine, and doxycycline. All data were analysed using independent t tests and the Bonferroni correction ($n = 10$; * $P < .05$).

μ M marimastat-treated, 4.80 ± 1.20 D ($P < .01$) for the 5 μ M batimastat-treated, 7.06 ± 1.36 D ($P = .02$) for the 200 μ M doxycycline-treated, and 8.29 ± 0.95 D ($P = .61$) for the 50 μ M minocycline-treated FD eyes (Fig. 4b). After 28 days of treatment, the changes in both parameters exhibited normal distributions (both $P > .15$ in Kolmogorov–Smirnov tests and $P < .05$ in ANOVA). The changes in refractive errors and AL were further analysed using a post hoc test (Tukey's test). The interocular differences between individual groups and the PBS-treated mice calculated using independent-sample t tests and the Bonferroni correction were 9.35 ± 1.51 D for the PBS-treated, 5.36 ± 1.25 D ($P < .001$) for the 1% atropine-treated, 4.45 ± 1.46 D ($P < .001$) for the 50 μ M marimastat-treated, 4.80 ± 1.20 D ($P < .001$) for the 5 μ M batimastat-treated, 7.06 ± 1.36 D ($P = .002$) for the 200 μ M doxycycline-treated, and $8.29 \pm$

0.95 D ($P = .8$) for the 50 μ M minocycline-treated FD eyes (Fig. 4b). The mean interocular refractive differences in C57BL/6 mice are listed in supplemental Table 3.

The changes in both refractive error and AL exhibited normal distributions (both $P > .15$ in Kolmogorov–Smirnov tests), and the changes in refractive errors and AL were further analysed using independent-sample t tests and the Bonferroni correction. The changes in refractive errors were as follows: -7.95 ± 2.05 D in PBS-treated, -4.94 ± 1.78 D in 1% atropine-treated, -4.75 ± 0.66 D in 50 μ M marimastat-treated, -5.14 ± 1.97 D in 5 μ M batimastat-treated, -5.72 ± 1.54 D in 200 μ M doxycycline-treated, and -6.38 ± 1.07 D in 50 μ M minocycline-treated FD eyes. The changes in refractive error were significant for the FD eyes treated with 1% atropine, 50 μ M marimastat, 5 μ M batimastat, and 200 μ M doxycycline

compared with those treated with PBS (all $P < .05$; Fig. 4c; the mean differences in refractive change between groups of C57BL/6 mice are listed in supplemental Table 4). The changes in AL were as follows: $208 \pm 56 \mu\text{m}$ in PBS-treated, $134 \pm 78 \mu\text{m}$ in 1% atropine-treated, $81 \pm 88 \mu\text{m}$ in 50 μM marimastat-treated, $118 \pm 60 \mu\text{m}$ in 5 μM batimastat-treated, $141 \pm 65 \mu\text{m}$ in 200 μM doxycycline-treated, and $151 \pm 54 \mu\text{m}$ in 50 μM minocycline-treated FD eyes. The changes in AL were significant for the FD eyes treated with 1% atropine, 50 μM marimastat, 5 μM batimastat, and 200 μM doxycycline compared with those treated with PBS (all $P < .05$; Fig. 4d; the mean differences in AL changes between groups of C57BL/6 mice are listed in supplemental Table 5).

After euthanasia and enucleation on day 28, the AL was $3.17 \pm 0.04 \text{ mm}$ in PBS-treated, $3.13 \pm 0.08 \text{ mm}$ in 1% atropine-treated, $3.12 \pm 0.05 \text{ mm}$ in 50 μM marimastat-treated, $3.10 \pm 0.05 \text{ mm}$ in 5 μM batimastat-treated, $3.12 \pm 0.03 \text{ mm}$ in 200 μM doxycycline-treated, and $3.13 \pm 0.03 \text{ mm}$ in 50 μM minocycline-treated FD eyes. The ALs of all treated eyes were thus shorter than those of the PBS-treated FD eyes (all $P < .05$). The interocular differences in AL (FD vs untreated eyes) on day 28 were $81.30 \pm 42.92 \mu\text{m}$ in PBS-treated, $30.00 \pm 28.68 \mu\text{m}$ in 1% atropine-treated, $40.75 \pm 28.98 \mu\text{m}$ in 50 μM marimastat-treated, $38.22 \pm 33.27 \mu\text{m}$ in 5 μM batimastat-treated, $41.10 \pm 34.79 \mu\text{m}$ in 200 μM doxycycline-treated and $43.89 \pm 23.12 \mu\text{m}$ in 50 μM minocycline-treated FD eyes. The AL differences between eyes in all drug-treated FD mice were smaller than those of the PBS-treated FD mice (all $P < .05$).

The changes in refractive error and AL between days 21 and 0 were measured in the hamster myopia model. The repeated measurement variability of AL was excellent (ICC = 0.89). After 21 days of treatment, the changes in refractive error were as follows: $-7.3 \pm 1.5 \text{ D}$ in PBS-treated, $-2.9 \pm 1.7 \text{ D}$ in 1% atropine-treated, $-3.6 \pm 1.5 \text{ D}$ in 50 μM marimastat-treated, $-3.8 \pm 1.6 \text{ D}$ in 5 μM batimastat-treated, and $-5.0 \pm 1.5 \text{ D}$ in 200 μM doxycycline-treated FD hamsters. All the changes were significant compared with that in the PBS-treated hamsters (all $P < .05$ after independent-sample t tests and the Bonferroni correction; Fig. 4e; the mean differences in refractive change between groups of hamsters are listed in supplemental Table 6). The changes in AL were as follows: $604 \pm 40 \mu\text{m}$ in PBS-treated, $333 \pm 27 \mu\text{m}$ in 1% atropine-treated, $343 \pm 25 \mu\text{m}$ in 50 μM marimastat-treated, $399 \pm 26 \mu\text{m}$ in 5 μM batimastat-treated, and $446 \pm 42 \mu\text{m}$ in 200 μM doxycycline-treated FD hamsters. All changes in the treated eyes of the FD hamsters compared with those in the PBS-treated FD hamsters were significant (all $P < .05$ after independent-sample t tests and the Bonferroni correction; Fig. 4f; the mean differences in AL change between groups of hamsters are listed in supplemental Table 7).

Scleral thickness and collagen fibril diameters in the C57BL/6 mouse myopia model

H&E-stained cross-sections of posterior scleras from left unoccluded eyes and FD right eyes are presented in Fig. 5a–f. The area of the sclera proximal to the optic nerve was defined as the posterior sclera. In particular, the posterior sclera of the FD PBS-treated eyes appeared visibly thinner (Fig. 5a). The mean thicknesses of the sclera treated with each compound were compared with that of the PBS-treated sclera by using independent-sample t tests and the Bonferroni correction and were as follows: $22.37 \pm 4.37 \mu\text{m}$ in unoccluded control eyes and $14.36 \pm 2.41 \mu\text{m}$ in PBS-treated, $18.70 \pm 1.58 \mu\text{m}$ in 1% atropine-treated ($P = .04$), $18.87 \pm 2.75 \mu\text{m}$ in 50 μM marimastat-treated ($P = .005$), $18.18 \pm 4.12 \mu\text{m}$ in 5 μM batimastat-treated ($P = .07$), $19.03 \pm 4.48 \mu\text{m}$ in 200 μM doxycycline-treated ($P = .04$), and $17.13 \pm 2.24 \mu\text{m}$ in 50 μM minocycline-treated FD eyes ($P = .10$; Fig. 5g). These results indicated that in eyes treated with 1% atropine, 50 μM marimastat, 5 μM batimastat, and 200 μM

doxycycline, scleral thinning resulting from FDM was impeded in C57BL/6 mice.

The collagen fibril structure of the posterior sclera was analysed using TEM at a high magnification (60 000 \times ; Fig. 6a–f). In the PBS-treated FD eyes, collagen lamellae were arranged relatively loosely and irregularly; the diameter of collagen fibrils was rather variable, and the percentage of small-diameter collagen fibrils was higher (Fig. 6a). By contrast, in FD eyes treated with 1% atropine, 50 μM marimastat, 5 μM batimastat, or 200 μM doxycycline, the distribution and arrangement of collagen fibrils were more homogenous (Fig. 6b–f). The mean collagen fibril diameters were as follows: $53.58 \pm 18.89 \text{ nm}$ in PBS-treated, $66.08 \pm 16.98 \text{ nm}$ in 1% atropine-treated, $63.18 \pm 17.89 \text{ nm}$ in 50 μM marimastat-treated, $57.34 \pm 17.45 \text{ nm}$ in 5 μM batimastat-treated, $58.40 \pm 17.82 \text{ nm}$ in 200 μM doxycycline-treated, and $54.22 \pm 15.62 \text{ nm}$ in 50 μM minocycline-treated FD eyes (all $P < .005$ compared with that of PBS-treated FD eyes with independent-sample t tests and the Bonferroni correction; Fig. 6g).

qRT-PCR, western blotting, and ELISA results for the C57BL/6 mouse myopia model

The qPCR, Western blotting, and ELISA results were analysed using independent-sample t tests and the Bonferroni correction. The relative gene expressions in PBS-treated right eyes and untreated left eyes, determined using qRT-PCR, are presented in Fig. 7a. The level of MMP-9 mRNA was higher and that of collagen 1 α mRNA was lower in the FD eyes. The levels of MMP-2, MMP-3, MMP-7, TIMP-2, and TGF- β mRNAs did not differ (Fig. 7a).

Levels of TGF- β 2 mRNA did not significantly change for any treatment compared with those in FD eyes treated with PBS (Fig. 7b). Levels of TIMP-2 mRNA were significantly lower in 5 μM batimastat-treated FD eyes than in PBS-treated FD eyes (Fig. 7c). Levels of MMP-2 mRNA were significantly lower in 50 μM marimastat-treated and 5 μM batimastat-treated FD eyes than in PBS-treated FD eyes (Fig. 7d). Levels of MMP-3 mRNA were lower in 50 μM marimastat-treated and 5 μM batimastat-treated FD eyes but significantly higher in 200 μM doxycycline-treated and 50 μM minocycline-treated FD eyes compared with PBS-treated FD eyes (Fig. 7e). Levels of MMP-7 mRNA were lower in 50 μM marimastat-treated FD eyes but higher in 50 μM minocycline-treated FD eyes compared with PBS-treated FD eyes (Fig. 7f). Significantly lower levels of MMP-9 mRNA were discovered in 5 μM batimastat-treated and 50 μM minocycline-treated FD eyes than in PBS-treated FD eyes (Fig. 7g). Collagen 1 α mRNA levels were significantly lower in 1% atropine-treated, 50 μM marimastat-treated, and 5 μM batimastat-treated FD eyes than in PBS-treated FD eyes (Fig. 7h). In Western blotting, the amount of each scleral protein, as revealed in western blots, was normalised to the amount of GAPDH in the same lane of the blot. Then, the normalized amount of scleral proteins in the compound-treated FD eyes was compared with those in PBS-treated FD eyes. The data were analysed using independent-sample t tests and the Bonferroni correction. The relative protein fold difference of TIMP-2, TGF- β 2, and TGF- β 3 did not significantly differ among treatments (Fig. 8a, c, h, and i; supplemental Fig. 1). The relative protein fold difference of MMP-2 was significantly lower in 1% atropine-treated, 50 μM marimastat-treated, 5 μM batimastat-treated, 200 μM doxycycline-treated, and 50 μM minocycline-treated FD eyes (all $P < .05$; Fig. 8d). The relative protein fold differences of MMP-3 decreased significantly in 200 μM doxycycline-treated and 50 μM minocycline-treated FD eyes (both $P < .05$; Fig. 8e). The relative protein fold difference of MMP-7 was significantly lower in 1% atropine-treated, 50 μM marimastat-treated, 5 μM batimastat-treated, and 200 μM doxycycline-treated FD eyes (all $P < .05$; Fig. 8f; supplemental Fig. 1). The relative protein fold difference of MMP-9 expression was significantly lower in 5 μM batimastat-treated and 200 μM doxycycline-treated FD eyes (both $P = .01$). A trend of higher

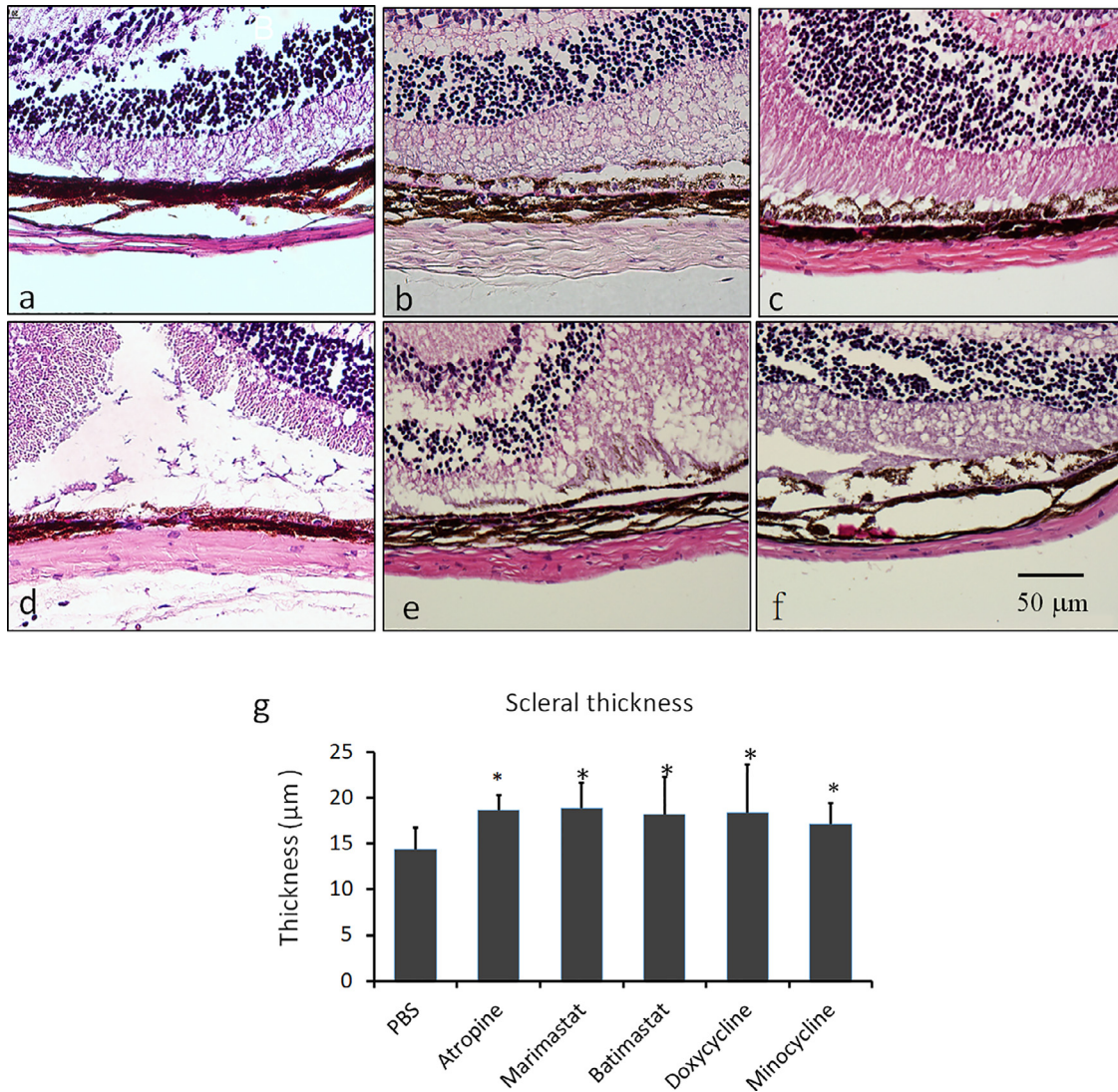


Fig. 5. Histology of the posterior sclera stained with H&E in FD C57BL/6 mouse eyes treated with (a) PBS, (b) 1% atropine, (c) 50 μM marimastat, (d) 5 μM batimastat, (e) 200 μM doxycycline, and (f) 50 μM minocycline. (g) Average scleral thickness in FD C57BL/6 mouse eyes treated with PBS, 1% atropine, 50 μM marimastat, 5 μM batimastat, 200 μM doxycycline, and 50 μM minocycline (* $P < .05$, $n = 10$).

relative protein expression of collagen $\alpha 1$ and $\alpha 2$ was found in 1% atropine-treated, 5 μM batimastat-treated, 50 μM marimastat-treated, and 200 μM doxycycline-treated FD eyes, but this result was nonsignificant except for the collagen $\alpha 2$ level in 5 μM batimastat-treated FD eyes (Fig. 8b). In sum, lower MMP-2 and MMP-7 expression was observed in most treatments. Downregulated MMP-3 and MMP-9 expression was observed in some treatments; however, this downregulation did not significantly increase the protein levels of collagen $\alpha 1$ and $\alpha 2$.

In the ELISA results total MMP activity was significantly lower in all groups than in PBS-treated FD eyes ($P < .01$; Fig. 9a). The relative fluorescence units (RFU) were used to express the enzymatic activity of MMPs (1 μg/ml in MMPs and 100 μg/ml in MMP-2 and MMP-9). The MMP-2 activity was 1.81 ± 0.32 RFU in 1% atropine-treated ($P = .18$), 1.37 ± 0.42 RFU in 50 μM marimastat-treated ($P = .18$), 1.43 ± 0.05 RFU in 5 μM batimastat-treated ($P = .01$), 1.40 ± 0.12 RFU in 200 μM doxycycline-treated ($P = .02$), and 1.42 ± 0.25 RFU in 50 μM minocycline-treated ($P = .12$) FD eyes compared with that in PBS-treated FD eyes (1.62 ± 0.07 RFU; Fig. 9b). The MMP-9 activity was 7.64 ± 3.38 RFU in 1% atropine-treated ($P = .12$), 7.67 ± 3.09 RFU in 50 μM marimastat-treated ($P = .11$), 6.08 ± 2.23 RFU in 5 μM batimastat-treated ($P = .01$), 6.88 ± 3.70 RFU in 200 μM

doxycycline-treated ($P = .08$), and 7.95 ± 2.95 RFU in 50 μM minocycline-treated ($P = 0.12$) FD eyes compared with that in PBS-treated FD eyes (10.05 ± 1.46 RFU; Fig. 9c).

Discussion

In the current study, we screened candidate compounds from an FDA-approved compound library for their ability to prevent myopia progression, and we validated the compounds' effectiveness in rodent FDM models. Our results are congruous with those of other studies, revealing that the upregulation of MMP expression is associated with the induction of myopic change [12–57]. Notably, this study confirmed the feasibility of the current strategy for screening candidate drugs and the MMP inhibitors that may be useful in preventing myopia development and progression.

Among the screened compounds and MMP inhibitors, batimastat (5 μM) and marimastat (50 μM) appeared the most effective in preventing the progression of FDM in rodents. However, three mouse eyes dosed with 50 μM marimastat ($n = 10$) and two mouse eyes dosed with 5 μM batimastat ($n = 10$) exhibited severe corneal toxicity, periocular skin swelling, and periocular hair loss. Furthermore, in both groups, one eye perforated in the fourth week of treatment. This

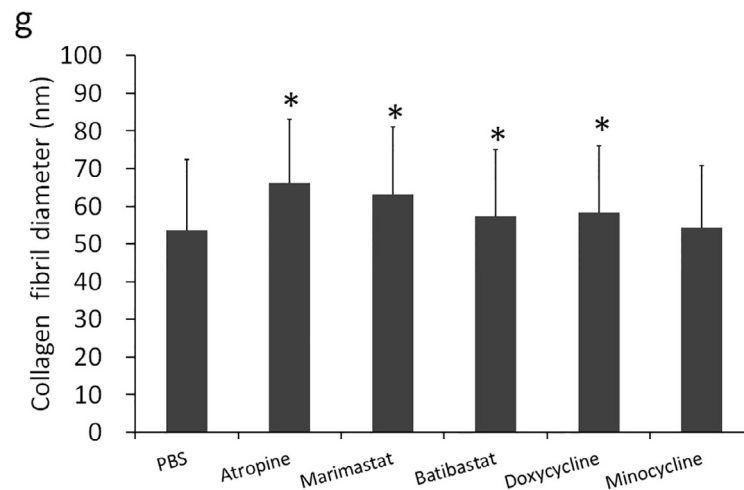
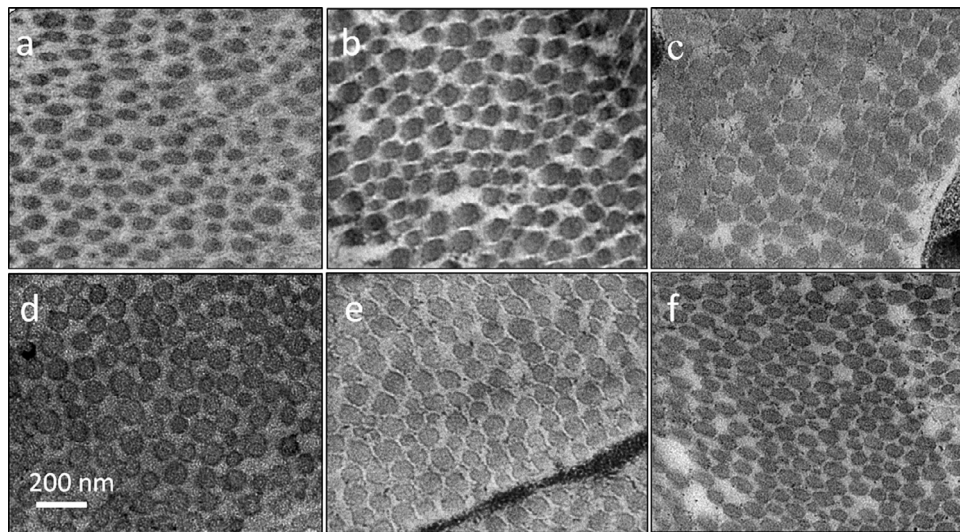


Fig. 6. TEM images showing collagen fibrils in the posterior sclera of FD C57BL/6 mice treated with (a) PBS, (b) 1% atropine, (c) 50 μ M marimastat, (d) 5 μ M batimastat, (e) 200 μ M doxycycline, and (f) 50 μ M minocycline. (g) Average collagen fibril diameter for treatment with 1% atropine, 50 μ M marimastat, 5 μ M batimastat, and 200 μ M doxycycline was significantly different from that for PBS treatment in FD C57BL/6 mouse eyes (* $P < .05$, $n = 10$).

side effect may be attributable to these compounds' corneal toxicity, which impaired normal corneal epithelial and stromal wound healing; nevertheless, further investigation is warranted. We do not believe that either compound can be applied in future clinical trials if they are this toxic. Doxycycline, by contrast, does not possess such toxicity and is an FDA-approved drug with a favourable safety profile [58]. Although the doxycycline-induced MMP inhibition was less pronounced than that induced by batimastat or marimastat, the capacity of doxycycline to mitigate myopia progression was comparable to that of atropine in rodent FDM.

Relative to the control left eyes, the FD right eyes treated with PBS had upregulation of TGF- β 2, TIMP-2, MMP-2, MMP-3, MMP-7, and MMP-9 mRNA; the findings of TGF- β 2 and TIMP-2 mRNA upregulation are inconsistent with those in previous reports [10, 57]. However, the upregulation of TGF- β 2 and TIMP-2 mRNA was nonsignificant; only the upregulation of MMP-9 and downregulation of collagen α 1 reached significance. Studies have identified the efficacy of doxycycline in ocular surface repair [59] and the treatment of recalcitrant corneal erosion, which are possibly attributable to its inhibitory effects on MMP-2 and MMP-9 [60]. Ex vivo studies of corneal epithelial cells have revealed that doxycycline does not appear to inhibit MMP synthesis directly but through the indirect inhibition of IL-1 α synthesis [61]. A study of human aortic smooth muscle cells

revealed that doxycycline at concentrations of 2.5 to 40 μ g/mL achieves inhibition by reducing MMP-2 mRNA stability or reducing the synthesis of MMP-2 and MMP-9 mRNA; at concentrations exceeding 50 μ g/mL in periodontal epithelial cells [62], doxycycline also inhibits enzymatic activity of MMPs by chelating metal ions to reduce their activity [63]. In the present study, doxycycline at 200 μ g/mL not only suppressed the expression of MMP-2 mRNA ($P = .04$) but also reduced the protein levels of latent forms of MMP-2 and MMP-9 and the enzymatic activity of MMP-2 and MMPs while having no effect on the expression of TIMP-2 and TGF- β . We ascribed the coexisting inhibition effects to the dilution of doxycycline solution in tears and aqueous humour and its uneven distribution in ocular tissues; thus, both types of inhibition occurred in our experiment [64, 65]. Therefore, we propose that doxycycline downregulates MMP-2 activity by reducing MMP-2 mRNA synthesis and chelating MMP-2 protein, but this speculation requires further investigation.

Scleral thinning in highly myopic human eyes was shown to be associated with the narrowing and dissociation of collagen fibril bundles and a reduction in collagen fibril diameter [66]. Chakravarti et al. found decreased scleral thickness and an increased number of small-diameter collagen fibrils in fibromodulin- and lumican-null 6-week-old C57BL/6 mice [15]. McBrien et al. examined collagen fibril architecture and scleral thinning in myopic tree shrews [67]. They found

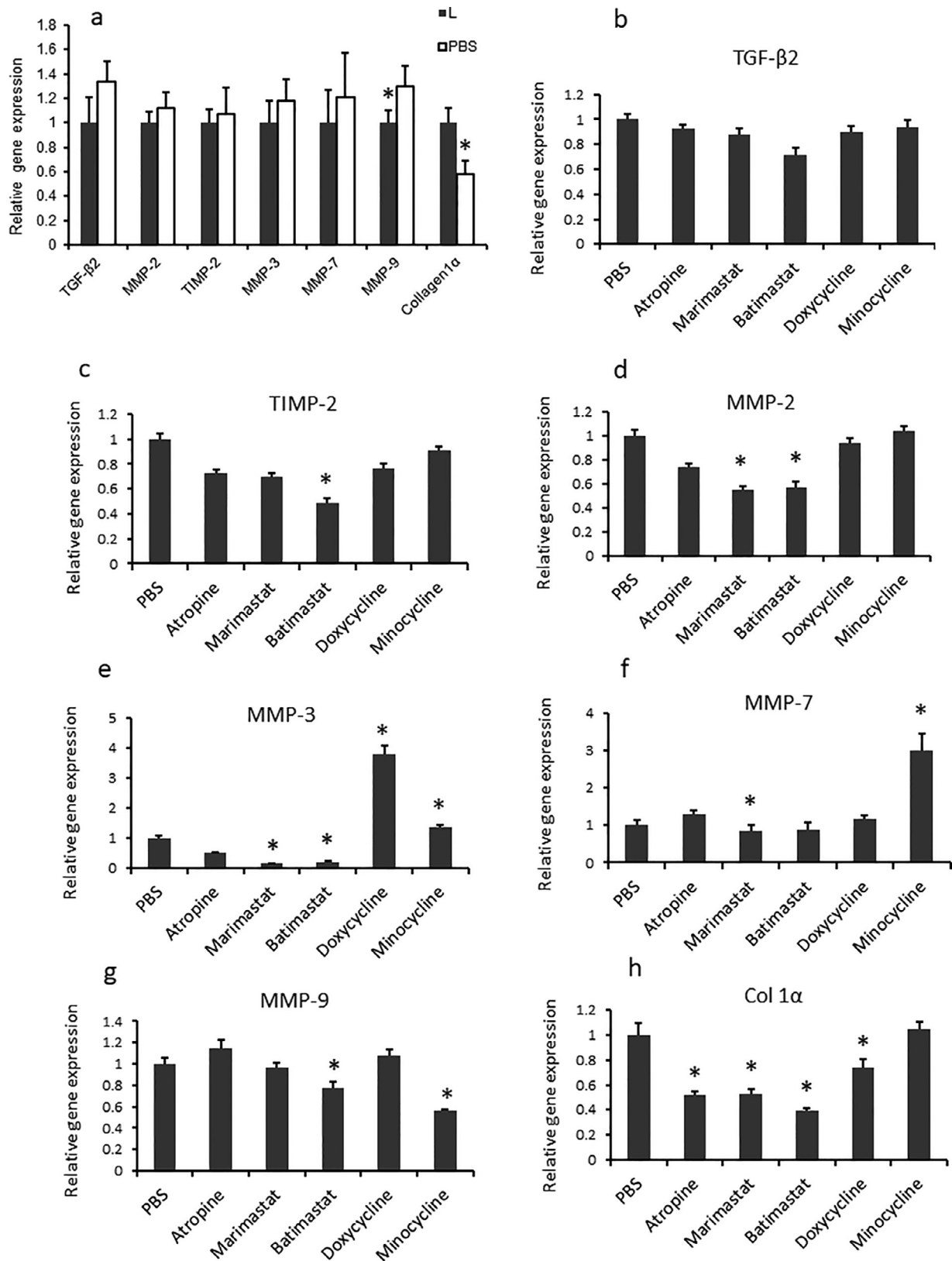


Fig. 7. Quantification of gene expression by qRT-PCR. (a) Upregulation of MMP-9 and downregulation of collagen 1 α in FD right eyes treated with PBS relative to left control eyes. Levels of mRNAs after treatment: (b) TGF- β 2, (c) TIMP-2, (d) MMP-2, (e) MMP-3, (f) MMP-7, and (g) MMP-9. Borderline significant downregulation of MMP-2 after treatment with 200 μ M doxycycline ($P = .08$). (h) The level of collagen 1 α mRNA was significantly downregulated after treatment with 1% atropine, 50 μ M marimastat, 5 μ M batimastat, or 200 μ M doxycycline (L: left control eyes; * $P < .05$; $n = 6$).

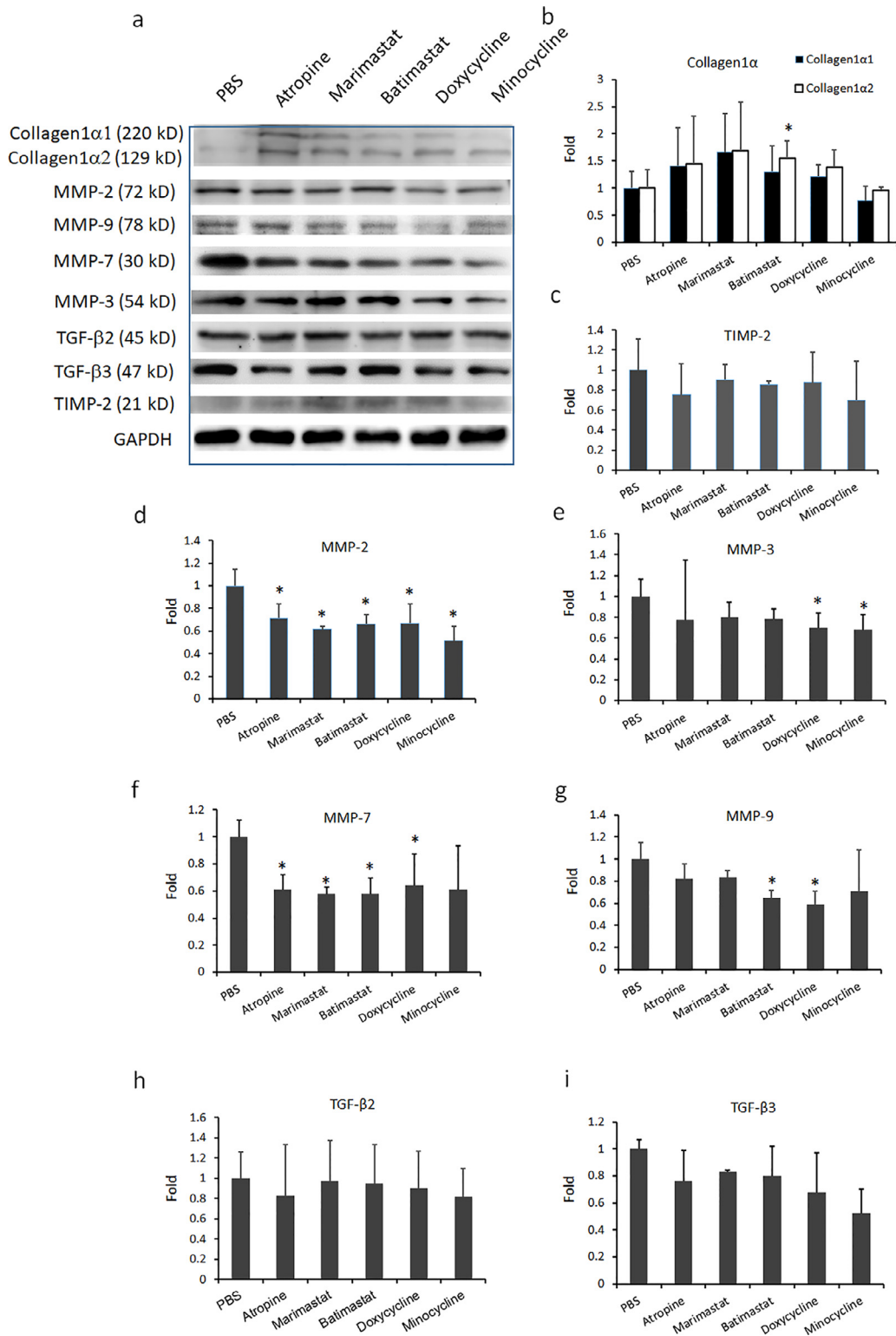


Fig. 8. (a) Western blot of scleral protein extracts. (b) After treatment with the compounds, the levels of collagen $\alpha 1$ and $\alpha 2$ tended to be elevated, although only the change in collagen $\alpha 2$ level was significant for the 5 μ M batimastat-treated eyes. The levels of (c) TIMP-2, (h) TGF- $\beta 2$, and (i) TGF- $\beta 3$ were not significantly different among treatments. (d–g) Levels of MMP-2, MMP-3, MMP-7, and MMP-9, respectively. MMP-2 and MMP-7 levels decreased significantly more than those of MMP-3 and MMP-9 did after treatment with 1% atropine and other MMP inhibitors (* $P < .05$; n = 6).

that scleral tissue loss and subsequent scleral thinning occurred rapidly (12 days) during the development of axial myopia, although the initial tissue loss was not accompanied by significant alterations of collagen fibril diameter distribution until 3 months into form deprivation. They ascribed the short-term tissue loss to general scleral collagen fibril degradation rather than to the degradation of fibrils of

certain diameters. In the current study, we determined that treatment with 1% atropine, 50 μ M marimastat, 5 μ M batimastat, or 200 μ M doxycycline mitigated scleral thinning caused by form deprivation. Treatment with atropine and these MMP inhibitors also reduced the percentage of small-diameter collagen fibrils and maintained the regularity of collagen fibrils, which is adversely affected by

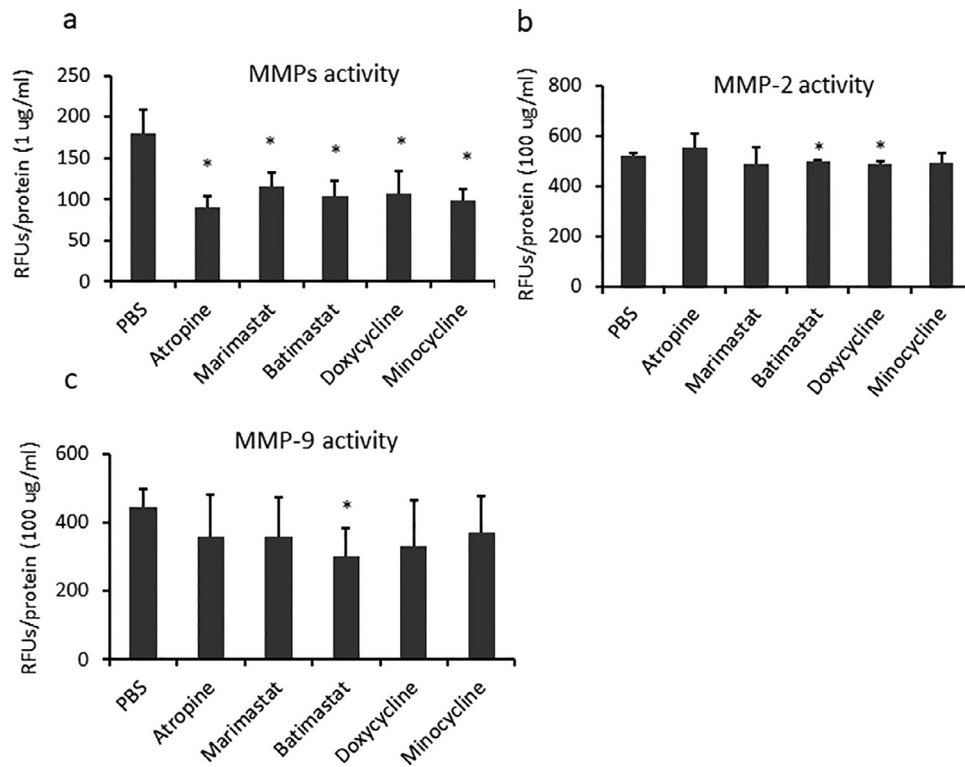


Fig. 9. Quantification of MMP activity using ELISA. (a) All MMP activity was significantly lower in eyes receiving treatments compared with PBS-treated FD eyes ($P < .01$). (b) MMP-2 activity was significantly downregulated in FD eyes treated with 5 μ M batimastat or 200 μ M doxycycline ($P < .05$). (c) MMP-9 activity was significantly downregulated in FD eyes treated with 5 μ M batimastat ($P = .01$; $n = 6$). The relative fluorescence units (RFU) were used to express the enzymatic activity of MMP (1 μ g/ml in MMPs and 100 μ g/ml in MMP-2 and MMP-9).

form deprivation. This is concordant with an earlier report that suggested that scleral thinning can occur prior to changes in collagen fibril diameter [67]. In the study by Chakravarti et al, collagen fibril changes were more prominent in lumican- and fibromodulin-null mice than in normal mice at the age of 6 weeks; however, the changes observed in the current study were not as great [15]. We attributed the differences to the potentially more dominant effect of genetic inheritance over that of external stimuli. In lumican- and fibromodulin-null mice, the expression of lumican and fibromodulin proteins, respectively, is diminished or absent from conception, whereas in the current study, form deprivation and the instillation of eye drops were imposed from 21 to 42 days after birth in hamsters and from 28 to 56 days after birth in mice. Although form deprivation can cause myopic changes and axial elongation, elevated MMP expression, smaller scleral thickness, and irregularly arranged and small-diameter collagen fibrils were all inhibited by treatment with 1% atropine, 50 μ M marimastat, 5 μ M batimastat, or 200 μ M doxycycline. In the effectively treated eyes, we identified a smaller myopic shift, less axial elongation, less scleral thinning, fewer small-diameter collagen fibrils, and downregulation of MMP gene and protein expression in the sclera, which is comparable to the changes being observed in atropine-treated group. MMP inhibitors such as marimastat, batimastat, and doxycycline can modify scleral remodelling biochemically, morphologically, and structurally, and these effects may be reflected in refractive and biometric changes.

The current study had limitations. First, refractive changes in the FDM of hamsters were smaller than those in C57BL/6 mice. We reasoned that this was because of the different methods and different periods of FDM induction. To induce FDM, we sutured diffusers for 28 days from 4 weeks old in mice, whereas in hamsters, we sutured eyelids for 21 days from 3 weeks old. Suturing the eyelid appeared flatten the corneal curvature [44–68]. This may have led to a different amount of myopic shift between both models, although significance

was reached in both animal models. In our experiment, ALs measured using ultrasound biomicroscopy were validated with direct measurements after enucleation; the measurements were compatible with those obtained using ultrasound biomicroscopy, as stated in the results. Furthermore, according to the schematic eye model in mice, the calculated axial eye elongation of 5.4–6.5 μ m corresponds to a 1-D myopic shift [49], in which the refractive status was measured using an eccentric infrared photorefractor. Tejedor et al. [44] and Qian et al. [69] used streak retinoscopy to study the refractive status of C57BL/6 mice and discovered a change in AL of 39 μ m/D and 8.9 μ m/D, respectively. In the current study, we also used streak retinoscopy and ultrasound biomicroscopy to measure the relative change in the refraction and AL in mice. We determined that the change in AL was 25 μ m/D, which was in the range of the values obtained in the other studies. However, some of the assumptions made in the paraxial model, such as the curvature or refractive index values, may have varied with different measuring tools, causing discrepancy. This can explain the discrepancy in the results between the current study and the schematic eye model. Although optical low-coherence interferometry [70] and real-time optical coherence tomography [71] data were unavailable in current study, we hope they can be used to confirm our results in the future. Finally, we employed an RS-MO that has been extensively used with few reports of off-target effects at reasonable doses [39], and which was the only *zlm* control morpholino available off-the-shelf. A scrambled sequence would be a better control than the random sequence, however, because it would have the same overall numbers of each nucleotide, and therefore, the same net charge and hydrophobicity, and the retina-specific effects in zebrafish cannot be excluded.

In conclusion, this study provides a useful strategy for screening candidate drugs and thus identifying compounds for clinical trials. We also demonstrated that MMP inhibitors, especially doxycycline, may mitigate axial myopic change, with suitable efficacy and toxicity,

in FD eyes in both C57BL/6 mice and golden Syrian hamsters. Doxycycline solution at 200 $\mu\text{g}/\text{mL}$ directly and indirectly reduced the amount of MMP-2 protein in the sclera by inhibiting MMP-2 gene expression, protein synthesis, or activity. Cross-species validation demonstrated that the agents may serve as an alternative to atropine and have fewer side effects and better therapeutic effects. However, clinical trials in humans are required to investigate this indication.

Funding sources

This research was supported by grants from Taiwan's Ministry of Science and Technology (NSC100-2314-B002-061-MY3, MOST105-2325-B002-037, MOST106-3114-B002-010, and MOST107-2321-B002-069) and Ministry of Health and Welfare (DOH100-TD-PB-111-TM005, DOH101-TD-PB-111-TM017, DOH102-TD-PB-111-TM013, MOHW103-TDU-PB-211-112015, and MOHW104-TDU-PB-211-122012).

Declaration of Competing Interest

The other authors declare no competing interests.

Conflict of Interest

All authors declare that they have no financial or commercial conflicts of interest.

Acknowledgements

We thank all participants of the current study. We also thank the staff of the Second Core Lab at the Department of Medical Research of National Taiwan University Hospital for their technical support.

Supplementary materials

Supplementary material associated with this article can be found, in the online version, at doi:[10.1016/j.ebiom.2021.103263](https://doi.org/10.1016/j.ebiom.2021.103263).

References

- [1] Rada JA, Shelton S, Norton TT. The sclera and myopia. *Exp Eye Res* 2006;82:185–200.
- [2] Norton TT, Rada JA. Reduced extracellular matrix in mammalian sclera with induced myopia. *Vision Res* 1995;35:1271–81.
- [3] Harper AR, Summers JA. The dynamic sclera: extracellular matrix remodeling in normal ocular growth and myopia development. *Exp Eye Res* 2015;133:100–11.
- [4] Nagase H, Visse R, Murphy G. Structure and function of matrix metalloproteinases and TIMPs. *Cardiovasc Res* 2006;69:562–73.
- [5] Phillips JR, Khalaj M, McBrien NA. Induced myopia associated with increased scleral creep in chick and tree shrew eyes. *Invest Ophthalmol Vis Sci* 2000;41:2028–34.
- [6] Siegwart JT, Jr, Norton TT. The time course of changes in mRNA levels in tree shrew sclera during induced myopia and recovery. *Invest Ophthalmol Vis Sci* 2002;43:2067–75.
- [7] Siegwart JT, Jr, Norton TT. Selective regulation of MMP and TIMP mRNA levels in tree shrew sclera during minus lens compensation and recovery. *Invest Ophthalmol Vis Sci* 2005;46:3484–92.
- [8] Jia Y, Hu DN, Zhu D, Zhang L, Gu P, Fan X, et al. MMP-2, MMP-3, TIMP-1, TIMP-2, and TIMP-3 protein levels in human aqueous humor: relationship with axial length. *Invest Ophthalmol Vis Sci* 2014;55:3922–8.
- [9] Jia Y, Hu DN, Zhou J. Human aqueous humor levels of TGF- β 2: relationship with axial length. *Biomed Res Int* 2014;2014:258591.
- [10] Rada JA, Perry CA, Slover ML, Achen VR. Gelatinase A and TIMP-2 expression in the fibrous sclera of myopic and recovering chick eyes. *Invest Ophthalmol Vis Sci* 1999;40:3091–9.
- [11] Guggenheim JA, McBrien NA. Form-deprivation myopia induces activation of scleral matrix metalloproteinase-2 in tree shrew. *Invest Ophthalmol Vis Sci* 1996;37:1380–5.
- [12] Zhao F, Zhou Q, Reinach PS, Yang J, Ma L, Wang X, et al. Cause and Effect Relationship between Changes in Scleral Matrix Metalloproteinase-2 Expression and Myopia Development in Mice. *Am J Pathol* 2018;188:1754–67.
- [13] Chen ZT, Wang JJ, Shih YF, Lin LL. The association of haplotype at the lumican gene with high myopia susceptibility in Taiwanese patients. *Ophthalmology* 2009;116:1920–7.
- [14] Majava M, Bishop PN, Hagg P, Scott PG, Rice A, Inglehearn C, et al. Novel mutations in the small leucine-rich repeat protein/proteoglycan (SLRP) genes in high myopia. *Hum Mutat* 2007;28:336–44.
- [15] Chakravarti S, Paul J, Roberts L, Chervoneva I, Oldberg A, Birk DE. Ocular and scleral alterations in gene-targeted lumican-fibromodulin double-null mice. *Invest Ophthalmol Vis Sci* 2003;44:2422–32.
- [16] Yeh LK, Liu CY, Kao WW, Huang CJ, Hu FR, Chien CL, et al. Knockdown of zebrafish lumican gene (*zlum*) causes scleral thinning and increased size of scleral coats. *J Biol Chem* 2010;285:28141–55.
- [17] Vutipongsatorn K, Yokoi T, Ohno-Matsui K. Current and emerging pharmaceutical interventions for myopia. *Br J Ophthalmol* 2019.
- [18] He M, Xiang F, Zeng Y, Mai J, Chen Q, Zhang J, et al. Effect of time spent outdoors at school on the development of myopia among children in china: a randomized clinical trial. *JAMA* 2015;314:1142–8.
- [19] Lipson MJ, Brooks MM, Koffler BH. The role of orthokeratology in myopia control: a review. *Eye Contact Lens* 2018;44:224–30.
- [20] Walline JJ, Lindsley K, Vedula SS, Cotter SA, Mutti DO, Twelker JD. Interventions to slow progression of myopia in children. *Cochrane Database Syst Rev* 2011; CD004916.
- [21] Bedrossian RH. The effect of atropine on myopia. *Ann Ophthalmol* 1971;3:891–7.
- [22] Siatkowski RM, Cotter S, Miller JM, Scher CA, Crockett RS, Novack GD. Safety and efficacy of 2% pirenzepine ophthalmic gel in children with myopia: a 1-year, multicenter, double-masked, placebo-controlled parallel study. *Arch Ophthalmol* 2004;122:1667–74.
- [23] Trier K, Olsen EB, Kobayashi T, Ribel-Madsen SM. Biochemical and ultrastructural changes in rabbit sclera after treatment with 7-methylxanthine, theobromine, acetazolamide, or L-ornithine. *Br J Ophthalmol* 1999;83:1370–5.
- [24] Hosaka A. Myopia prevention and therapy. The role of pharmaceutical agents. Japanese studies. *Acta Ophthalmol Suppl* 1988;185:130–1.
- [25] Chou AC, Shih YF, Ho TC, Lin LL. The effectiveness of 0.5% atropine in controlling high myopia in children. *J Ocul Pharmacol Ther* 1997;13:61–7.
- [26] O'Connor PS, Mumma JV. Atropine toxicity. *Am J Ophthalmol* 1985;99:613–4.
- [27] Chua WH, Balakrishnan V, Chan YH, Tong L, Ling Y, Quah BL, et al. Atropine for the treatment of childhood myopia. *Ophthalmology* 2006;113:2285–91.
- [28] Accessed September 8, 2019. <https://clinicaltrials.gov/ct2/show/NCT03140358>. Available from: <https://clinicaltrials.gov/ct2/show/NCT03140358>.
- [29] Chia A, Lu QS, Tan D. Five-year clinical trial on atropine for the treatment of myopia 2: myopia control with atropine 0.01% eyedrops. *Ophthalmology* 2016;123:391–9.
- [30] Accessed September 8, 2019. <https://clinicaltrials.gov/show/NCT02955927>. Available from: <https://clinicaltrials.gov/show/NCT02955927>.
- [31] Yam JC, Jiang Y, Tang SM, Law AKP, Chan JJ, Wong E, et al. Low-concentration atropine for myopia progression (LAMP) study: a randomized, double-blinded, placebo-controlled trial of 0.05%, 0.025%, and 0.01% atropine eye drops in myopia control. *Ophthalmology* 2019;126:113–24.
- [32] Schaeffel F. [Biological mechanisms of myopia]. *Ophthalmologie* 2017;114:5–19.
- [33] Shih YF, Chen CH, Chou AC, Ho TC, Lin LL, Hung PT. Effects of different concentrations of atropine on controlling myopia in myopic children. *J Ocul Pharmacol Ther* 1999;15:85–90.
- [34] Shih YF, Hsiao CK, Chen CJ, Chang CW, Hung PT, Lin LL. An intervention trial on efficacy of atropine and multi-focal glasses in controlling myopic progression. *Acta Ophthalmol Scand* 2001;79:233–6.
- [35] Tkatchenko TV, Shen Y, Tkatchenko AV. Mouse experimental myopia has features of primate myopia. *Invest Ophthalmol Vis Sci* 2010;51:1297–303.
- [36] Soules KA, Link BA. Morphogenesis of the anterior segment in the zebrafish eye. *BMC Dev Biol* 2005;5:12.
- [37] Kimmel CB, Ballard WW, Kimmel SR, Ullmann B, Schilling TF. Stages of embryonic development of the zebrafish. *Dev Dyn* 1995;203:253–310.
- [38] Westerfield M. The zebrafish book; a guide for the laboratory use of Zebrafish (*Brachydanio rerio*). 2nd edition Eugene: University of Oregon Press; 1993. p. 300P.
- [39] Nasevicius A, Ekker SC. Effective targeted gene 'knockdown' in zebrafish. *Nat Genet* 2000;26:216–20.
- [40] Thisse C, Thisse B. High-resolution in situ hybridization to whole-mount zebrafish embryos. *Nat Protoc* 2008;3:59–69.
- [41] Liu HH, Gentle A, Jobling AI, McBrien NA. Inhibition of matrix metalloproteinase activity in the chick sclera and its effect on myopia development. *Invest Ophthalmol Vis Sci* 2010;51:2865–71.
- [42] Ho WT, Chang JS, Su CC, Chang SW, Hu FR, Jou TS, et al. Inhibition of matrix metalloproteinase activity reverses corneal endothelial-mesenchymal transition. *Am J Pathol* 2015;185:2158–67.
- [43] Su W, Li Z, Li F, Chen X, Wan Q, Liang D. Doxycycline-mediated inhibition of corneal angiogenesis: an MMP-independent mechanism. *Invest Ophthalmol Vis Sci* 2013;54:783–8.
- [44] Tejedor J, de la Villa P. Refractive changes induced by form deprivation in the mouse eye. *Invest Ophthalmol Vis Sci* 2003;44:32–6.
- [45] Schaeffel F, Burkhardt E. Measurement of Refractive State and Deprivation Myopia in a Black Wildtype Mouse. *Invest Ophthalmol Vis Sci* 2002;43:182.
- [46] Barathi VA, Beuerman RW, Schaeffel F. Effects of unilateral topical atropine on binocular pupil responses and eye growth in mice. *Vision Res* 2009;49:383–7.
- [47] Barathi VA, Beuerman RW. Molecular mechanisms of muscarinic receptors in mouse scleral fibroblasts: Prior to and after induction of experimental myopia with atropine treatment. *Mol Vis* 2011;17:680–92.
- [48] Blehm C, Potvin R. Pseudophakic astigmatism reduction with femtosecond laser-assisted corneal arcuate incisions: a pilot study. *Clin Ophthalmol (Auckland, NZ)* 2017;11:201–7.

- [49] Schmucker C, Schaeffel F. A paraxial schematic eye model for the growing C57BL/6 mouse. *Vision Res* 2004;44:1857–67.
- [50] Lin HJ, Wei CC, Chang CY, Chen TH, Hsu YA, Hsieh YC, et al. Role of Chronic Inflammation in Myopia Progression: Clinical Evidence and Experimental Validation. *EBioMedicine* 2016;10:269–81.
- [51] Keller KE, Yang YF, Sun YY, Sykes R, Gaudette ND, Samples JR, et al. Interleukin-20 receptor expression in the trabecular meshwork and its implication in glaucoma. *J Ocul Pharmacol Ther* 2014;30:267–76.
- [52] Yang YF, Sun YY, Acott TS, Keller KE. Effects of induction and inhibition of matrix cross-linking on remodeling of the aqueous outflow resistance by ocular trabecular meshwork cells. *Sci Rep* 2016;6:30505.
- [53] Pifer MA, Maerz T, Baker KC, Anderson K. Matrix metalloproteinase content and activity in low-platelet, low-leukocyte and high-platelet, high-leukocyte platelet rich plasma (PRP) and the biologic response to PRP by human ligament fibroblasts. *The American journal of sports medicine* 2014;42:1211–8.
- [54] Koo TK, Li MY. A guideline of selecting and reporting intraclass correlation coefficients for reliability research. *J Chiropr Med* 2016;15:155–63.
- [55] Saika S, Shiraishi A, Liu CY, Funderburgh JL, Kao CW, Converse RL, et al. Role of lumican in the corneal epithelium during wound healing. *J Biol Chem* 2000;275:2607–12.
- [56] Grossniklaus HE, Green WR. Pathologic findings in pathologic myopia. *Retina* 1992;12:127–33.
- [57] McBrien NA. Regulation of scleral metabolism in myopia and the role of transforming growth factor-beta. *Exp Eye Res* 2013;114:128–40.
- [58] Sloan B, Scheinfeld N. The use and safety of doxycycline hyclate and other second-generation tetracyclines. *Expert Opin Drug Saf* 2008;7:571–7.
- [59] Smith VA, Cook SD. Doxycycline—a role in ocular surface repair. *Br J Ophthalmol* 2004;88:619–25.
- [60] Dursun D, Kim MC, Solomon A, Pflugfelder SC. Treatment of recalcitrant recurrent corneal erosions with inhibitors of matrix metalloproteinase-9, doxycycline and corticosteroids. *Am J Ophthalmol* 2001;132:8–13.
- [61] Solomon A, Rosenblatt M, Li DQ, Liu Z, Monroy D, Ji Z, et al. Doxycycline inhibition of interleukin-1 in the corneal epithelium. *Invest Ophthalmol Vis Sci* 2000;41:2544–57.
- [62] Liu J, Xiong W, Baca-Regen L, Nagase H, Baxter BT. Mechanism of inhibition of matrix metalloproteinase-2 expression by doxycycline in human aortic smooth muscle cells. *J Vasc Surg* 2003;38:1376–83.
- [63] Nip LH, Uitto VJ, Golub LM. Inhibition of epithelial cell matrix metalloproteinases by tetracyclines. *J Periodontol Res* 1993;28:379–85.
- [64] Salminen L. Penetration of ocular compartments by tetracyclines. II. An experimental study with doxycycline. *Albrecht Von Graefes Arch Klin Exp Ophthalmol*. 1977;204:201–207.
- [65] Kulshrestha OP, Kurian Keshwan, HH. Penetration of doxycycline in aqueous humour. (After oral administration in humans). *Indian J Ophthalmol* 1981;29:251–2.
- [66] Curtin BJ, Iwamoto T, Renaldo DP. Normal and staphylococcal sclera of high myopia. An electron microscopic study. *Arch Ophthalmol* 1979;97:912–5.
- [67] McBrien NA, Cornell LM, Gentle A. Structural and ultrastructural changes to the sclera in a mammalian model of high myopia. *Invest Ophthalmol Vis Sci* 2001;42:2179–87.
- [68] McBrien NA, Norton TT. The development of experimental myopia and ocular component dimensions in monocularly lid-sutured tree shrews (*Tupaia belangeri*). *Vision Res* 1992;32:843–52.
- [69] Qian YS, Chu RY, Hu M, Hoffman MR. Sonic hedgehog expression and its role in form-deprivation myopia in mice. *Curr Eye Res* 2009;34:623–35.
- [70] Schmucker C, Schaeffel F. In vivo biometry in the mouse eye with low coherence interferometry. *Vision Res* 2004;44:2445–56.
- [71] Zhou X, Xie J, Shen M, Wang J, Jiang L, Qu J, et al. Biometric measurement of the mouse eye using optical coherence tomography with focal plane advancement. *Vision Res* 2008;48:1137–43.